Proteomic characterization of Withaferin A-targeted protein networks for the treatment of monoclonal myeloma gammopathies

Accepted Manuscript

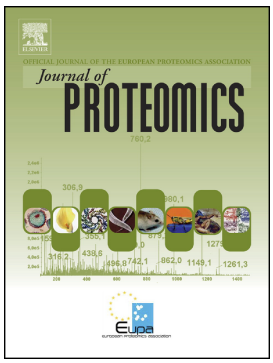

Proteomic characterization of Withaferin A-targeted protein networks for the treatment of monoclonal myeloma gammopathies

Martin Dom, Fritz Offner, Wim Vanden Berghe, Xaveer Van Ostade

PII: S1874-3919(18)30061-7
DOI: https://doi.org/10.1016/j.jprot.2018.02.013
Reference: JPROT 3044

To appear in: *Journal of Proteomics*

Received date: 23 August 2017
Revised date: 9 January 2018
Accepted date: 5 February 2018

Please cite this article as: Martin Dom, Fritz Offner, Wim Vanden Berghe, Xaveer Van Ostade , Proteomic characterization of Withaferin A-targeted protein networks for the treatment of monoclonal myeloma gammopathies. The address for the corresponding author was captured as affiliation for all authors. Please check if appropriate. Jprot(2017), https://doi.org/10.1016/j.jprot.2018.02.013

Proteomic characterization of Withaferin A-targeted protein networks for the treatment of monoclonal myeloma gammopathies

Martin Dom[1,2], Fritz Offner[2], Wim Vanden Berghe[1], Xaveer Van Ostade[1]*

[1]*Laboratory of Protein Chemistry, Proteomics and Epigenetic Signalling (PPES), Department of Biomedical Sciences, University of Antwerp (UA), Belgium*

[2]*Hematology, Department Internal Medicine, Ghent University, Ghent, Belgium*

Keywords: Withaferin A; Quantitative Chemoproteomics; Quantitative Proteomics; Multiple Myeloma; Waldenström Macroglobulinemia; Pathway Analysis

[*]**Corresponding author:** Xaveer Van Ostade, University of Antwerp, Universiteitsplein 1, 2610 Wilrijk (Belgium). Phone: +3232562319; email: xaveervanostade@uantwerpen.be

Conflict of interest: The authors declare no potential conflicts of interest.

Financial support: This research was supported by FWO grants G059713N and G079614N and the UA grant NOI/DOCPRO.

Data are available via ProteomeXchange with identifier PXD006528

Username: reviewer87960@ebi.ac.uk

Password: bCs1OLio

Abstract

Withaferin A (WA), a natural steroid lactone from the plant *Withania Somnifera*, is often studied because of its antitumor properties. Although many *in vitro* and *in vivo* studies have been performed, the identification of Withaferin A protein targets and its mechanism of antitumor action remains incomplete. We used quantitative chemoproteomics and differential protein expression analysis to characterize the WA antitumor effects on a multiple myeloma cell model. Identified relevant targets were further validated by Ingenuity Pathway Analysis and Western blot and indicate that WA targets protein networks that are specific for monoclonal gammopathy of undetermined significance (MGUS) and other closely related disorders, such as multiple myeloma (MM) and Waldenström macroglobulinemia (WM). By blocking the PSMB10 proteasome subunit, downregulation of ANXA4, potential association with HDAC6 and upregulation of HMOX1, WA puts a massive blockage on both proteotoxic and oxidative stress responses pathways, leaving cancer cells defenseless against WA induced stresses. These results indicate that WA mediated apoptosis is preceded by simultaneous targeting of cellular stress response pathways like proteasome degradation, autophagy and unfolded protein stress response and thus suggests that WA can be used as an effective treatment for MGUS and other closely related disorders.

Introduction

Despite progress and success in chemotherapy, many types of cancer remain largely incurable. One of the reasons for this lack of success is the development of (multi)drug resistance, characterized by cancer cells that manage to withstand the most powerful chemotherapies available [1,2]. It has been shown that tumors have developed a dynamic survival strategy by consisting of a very heterogeneous population of cancer cells [3,4] from which some can become resistant cells. In this respect, interest has recently focused on multifunctional chemotherapeutic compounds that simultaneously target a series of signaling networks that are necessary for cancer to develop [5–7]. Withaferin A (WA), a natural steroid lactone, is such a multifunctional compound with not only promising antitumor activity [8] but also anti-angiogenesis activity [9,10], anti-inflammatory activity [11,12], anti-metastatic activity [13] and re-sensitizing responses [14]. Remarkably, the steroid lactone Withanone (WN) has little or no proven antitumor effects [15], although it has the same chemical brute formula ($C_{28}H_{38}O_6$) and the same functional groups as WA (figure 1).

Currently, the *in vitro* antitumor mechanisms of WA include (I) changing the cytoskeleton architecture by binding vimentin [9,16], annexin A2 [17,18] and β-tubulin [19]; (II) inducing apoptosis by generating ROS [20–22]; (III) activating the pro-apoptotic protein Par-4 [23,24] and downregulating the anti-apoptotic protein Bcl-2 [25]; (IV) inhibiting proteasomes [26,27]; (V) suppressing NF-kB [12,28] and STAT3 [29]; (VI) downregulating ER-α [30]; and (VII) G2-M cell cycle arrest [13]. Additionally, antitumor activities of WA have been confirmed in several *in vivo* studies of different tumor models [31].

Although the above studies have help establish that WA has great promise as a novel chemotherapeutic, concerns have been raised about potential non-specific toxic side effects associated with WA, which hampers its further clinical development. For instance, WA binds with different filament systems, such as the intermediate filament protein vimentin and the microtubules protein β-tubulin. These cytoskeleton proteins are ubiquitously expressed and could hamper the

specificity of WA in clinical use. Therefore, it is of utmost importance to characterize the antitumor effects of WA on a proteome-wide scale to identify the most selective cancer targets for further preclinical drug optimization, with reduced side effects and limited multidrug resistance development.

For a global understanding of the antitumor effects of WA, we applied proteome-wide approaches to characterize direct and indirect antitumor effects of WA using quantitative chemoproteomics and quantitative shotgun strategy, respectively. For this analysis, we used an *in vitro* multiple myeloma (MM) model system consisting of MM1R and MM1S cells, which can be distinguished based on their sensitivity to steroid hormones such as glucocorticoids (GCs). MM is a clonal B-cell malignancy characterized by the accumulation of malignant plasma cells within the bone marrow [32]. MM is an incurable disease, and patients afflicted by this disease undergo subsequent phases of remission and relapse. Eventually this disease leads to multidrug resistance against all available drugs, such as glucocorticoids [33] and bortezomib [34],[35], and finally, death. Interestingly, WA has profound *in vitro* antitumor activity against multiple myeloma cells [29,36]. Therefore, elucidating this antitumor mechanism could provide us with valuable information regarding which crucial pathways must be targeted to efficiently inhibit multiple myeloma growth. This knowledge may pave the way towards new WA analogs and/or drugs that mimic (part of) the antitumor activity of WA.

Using MM1R cells, we identified 208 specific WA target proteins and 143 differentially expressed proteins. The integration of both datasets using Ingenuity Pathway Analysis (IPA) has resulted in the first global overview of WA and its molecular antitumor mechanism in multiple myeloma cells.

Materials and methods

Cell culture & reagents

All materials were purchased from Life Technologies unless stated otherwise. MM1R cells (CRL-2975), purchased from ATCC® (www.atcc.org), were cultured in RPMI-1640 complete medium (5%

penicillin/streptomycin, 10% fetal calf serum, 100X non-essential amino acids and 100X sodium pyruvate) at 37°C and 5% CO_2. For SILAC (stable isotope-labeled amino acid) experiments, an arginine- and lysine-depleted complete RPMI-1640 medium was used. SILAC stock solutions were prepared by dissolving $^{13}C_6$ L-Lysine-2HCl and $^{13}C_6$ L-Arginine-HCl in PBS, sterile filtering this solution through a 0.22 µm syringe filter and adding $^{13}C_6$ Lys and $^{13}C_6$ Arg to final concentrations of 23.2 mg/ml and 49.6 mg/ml, respectively, in the RPMI-1640 SILAC medium. Light stock solutions were prepared the same way, while extrapolating to maintain equimolar amounts of amino acids. Mass spectrometry validated that 5 cell doublings resulted in > 98% incorporation of these labels. Testing for mycoplasma was accomplished using a MycoAlert™ mycoplasma detection kit (LT07-418 Lonza).

Incubation and cell lysis

For quantitative chemoproteomic analysis, $8x10^7$ MM1R cells were treated for 3 h with 1 µM Withaferin A (WA) (AltaVista Phytochemicals, Telangana, India) or 1 µM biotinylated Withaferin A (WABI, figure 2, synthesized by Dr. Vander Veken, Universiteit Antwerpen). Next, $4x10^7$ cells of both WA- and WABI-stimulated MM1R cells were lysed (1 ml PBS + complete protease cocktail inhibitor (Roche)) by 3 freeze-thaw cycles. An overnight acetone precipitation (6X volume, -20°C) was performed to extract proteins. For further simultaneous analysis, 1 mg of total protein from each starting condition was pooled together. For the quantitative shotgun analysis, $8x10^7$ MM1R cells were treated with 1 µM WA or 1 µM Withanone (WN) (AltaVista Phytochemicals, Telangana, India) for 3 h and processed as described above. Accurate protein concentrations were determined using RP C4 HPLC. Our experience is that this method is more reproducible compared to Bradford or BCA probably because most impurities do not bind C4 and are washed from the column before elution of proteins and measurement of the area under the curve (AUC) value at 214 nm.

Streptavidin-biotin pull down

Enrichment of WABI-bound proteins was performed using Streptavidin Ultralink Resin (Thermo Fisher). First, 50µl of beads was washed 3 times with incubation buffer (5 mM Tris (pH 7.5), 50 mM

NaF, 5 mM EDTA and 1% Triton X-100) and incubated with 2 mg of the re suspended aceton-precipitated pellet in incubation buffer for 45 min on a turning wheel at room temperature. The beads were washed 2 times with incubation buffer and 3 times with PBS.

Western Blot

Briefly, SDS-PAGE was run, and proteins were transferred to a nitrocellulose membrane. Blocking was performed with 2% bovine serum albumin (BSA) for 1 h, and primary antibodies were incubated overnight. The primary antibodies used were as follows: anti-streptavidin-HRP (N100, Invitrogen), anti-ubiquitin (sc-8017, Santa Cruz), anti-annexin A4 (CSB-PA001845ESR2HU, CusaBio), anti-heme oxygenase 1 (P249, Cell Signaling), anti-caspase-3 (9662, Cell Signaling), anti-GAPDH (CSB-MA000071M0), anti-PSMB10 (sc-133236, Santa Cruz) and anti-PARP (H-250 sc-7150, Santa Cruz). The secondary antibodies used were as follows: goat anti-rabbit (D0487, Dako) and goat anti-mouse (Z0420, Dako).

On-bead trypsin digest

The washed beads were incubated for 1 h at 65°C (25 µl/100 µg protein) with a solution of 50 mM Tris (pH 8.7), 6 M urea, 5 mM DTT and 10% beta-mercaptoethanol. The samples were then diluted by adding 50 mM Tris (pH 8.7) and 1 mM $CaCl_2$ (75 µl/100 µg). Next, the proteins were alkylated by adding 200 mM iodoacetamide (10 µl/100 µg) and then stored in the dark for 1 h at 21°C. Finally, 13 µg of trypsin (proteomics grade, Roche) was added at a 30:1 protein-enzyme ratio and the mixture was incubated for 18 h at 37°C. Digestion was stopped by freezing (-20°C).

In-solution digest

In-solution digests were performed using the same protocol used for the on-bead digests starting with 2 mg of total protein content.

2D Liquid Chromatography

Peptides resulting from the on-bead and in-solution digests were separated in 2 dimensions. All solvents were LC-MS grade (Biosolve, Valkenswaard, Netherlands).

First dimension

In the first dimension, peptides were separated using a Reverse Phase C18 high pH ((X!Select CSH, RP-C18, 2.1 x 150 mm, 3.5 µm, Waters) column with an Alliance e2692 system (Waters Corporation, Milford, MA, USA). Solvent A (200 mM ammonium formate (pH 10)), Solvent B (100% water) and Solvent C (100% ACN) were applied in the following ACN gradient with a constant flow rate of 200 µl/min and continuously pumping 10% solvent A to have an overall pH of 10 during the entire run: 5% to 15% C in the first 5 min, 15% to 40% C in 80 min, 40% to 90% C in 8 min, 5 min at 90% C and 90% to 5% C in 2 min. Briefly, 30 fractions were collected from minute 10 till 100 with a 3 minute interval and all fractions were lyophilized to dryness and suspended in 97% H_20/3% ACN + 0.1% FA. Peptide concentrations were determined via the AUC values at 214 nm.

Second dimension for MALDI TOF/TOF

Briefly, 10 µg of each fraction was separated by reversed-phase chromatography in a second dimension on an Agilent 1100 micro-capillary HPLC system (Agilent Technologies, Waldbronn, Germany) as described previously [37].

Second dimension for Orbitrap Velos LTQ

For the LTQ Orbitrap Velos (Thermo Scientific, San Jose, CA, USA) analysis, the 30 peptide fractions from the first dimension were combined in a concatenated manner (e.g., fractions 1, 11 and 21) resulting in 10 fractions of which 1µg peptide mixture was separated in the second dimension by nano-reverse phase chromatography using an Acclaim C18 PepMap100 nano-Trap column (200 µm x 20 mm, 5 µm particle size) connected to an Acclaim C18 analytical column (75 µm x 150 mm, 3 µm particle size) (Thermo Scientific, San Jose, CA) on a Waters Nano ACQUITY UPLC system (Waters Corporation, Milford, MA, USA). The following gradient was used with solvent A (0.1%FA in 98%

$H_2$0/2% ACN) and B (0.1% FA in 2% $H_2$0/98% ACN) and a constant flow rate of 400 nl/min: 1%-5%B in 4 min, 5% - 20%B in 31 min, 20% - 40%B in 60 min, 40% -70%B in 7 min, 70% - 95%B in 3 min, 95% - 99%B in 3 min and back to equilibrating conditions of 1%B for 10 minutes. The nano-LC system was coupled online with the LTQ Orbitrap Velos using a PicoTip Emitter (New Objective, Woburn, MA) coupled to a nanospray ion source.

Mass Spectrometry

MALDI-TOF-TOF MS/MS analysis

Measurements were performed on an AB 4800 Plus MALDI-TOF/TOF analyzer (ABSciex, Nieuwerkerk aan den Ijssel, Netherlands) as described previously [37].

Orbitrap Velos LTQ analysis

The Orbitrap Velos LTQ (Thermo Scientific, San Jose, California) was used in the data-dependent mode. First, an MS precursor scan was performed in the mass range of 350 – 5000 m/z with a resolution of 60000. For each MS scan, the twenty most intense precursor peptide ions were selected for collision induced dissociation (CID). The CID scans were acquired in the LTQ ion trap of the mass spectrometer.

Data analysis

MALDI – TOF/TOF

Screening of the raw MS/MS data was performed with the Mascot search engine (Matrix Science, version 2.1.03) against the *Homo sapiens* database (UniProt ID proteome ID UP000005640). Database searches were performed using the digestion enzyme trypsin and a maximum of 2 missed trypsin cleavages was allowed. Carbamidomethylated cysteines were denoted as fixed modifications and oxidized methionine's as well as R6 and K6 heavy isotopes were denoted as variable modifications. Mass tolerances were set to 200 ppm and 0.2 Da for precursor and fragment ions, respectively. False discovery rate (FDR) was determined by Mascot according to [38]. A protein FDR <

5% was considered relevant. Additionally, peptide and protein identifications were further validated for their probability rates at ≥ 95% protein – and peptide confidence using Scaffold Q+ (Scaffold 4.0.5, Proteome Software Inc., Portland, Oregon) with the stringent protein prophet algorithm. After lowering the peptide threshold to 50%, WA target identifications that were based on 1 peptide underwent further quality control. They were tolerated when no counterpart light or heavy peptides (see figure 4C) were assigned at the lower (50%) peptide confidence. SILAC differential expression ratios were calculated with ProteinPilot (ProteinPilot Software 4.0, Applied Biosystems, Nieuwerkerk aan den Ijssel, Netherlands) according to the Paragon Algorithm with an additional FDR calculated via a nonlinear fitting method [39]. A global FDR of 1% and a local FDR of 5% was used. Only proteins with a ≥ 2-fold threshold change ratio were considered differentially regulated. Because of Scaffold stringency, only proteins that were identified in Scaffold were subsequently quantified in ProteinPilot and proteins that were quantified based on 1 peptide were manually excluded.

Orbitrap Velos LTQ

Raw data were converted by the Proteome Discoverer software (Thermo Scientific, San Jose, California) and screened against the *Homo sapiens* database (UniProt ID proteome ID UP000005640) using the Mascot search engine (Matrix Science, version 2.1.03). Database searches were performed similarly to the MALDI analysis, except mass tolerances were set to 10 ppm and 0.5 Da for precursor and fragment ions, respectively. SILAC differential expression ratios were calculated with PEAKS 7 software (Bioinformatics Solutions Inc, Waterloo, Ontario, Canada) and proteins were only accepted if the fold change ratio was ≥ 2 and the standard deviation (SD), related to the abundance ratio of protein expression, ≠ 0. This way, we automatically selected for proteins that were quantified on the basis of more than one peptide. An additional FDR curve was estimated with the decoy fusion method. All ≥ 2 fold differential expressed proteins have a -10lgP value > 40, corresponding with a protein false discovery rate (FDR) < 2.5%. Because of Scaffold stringency, only proteins that were identified in Scaffold were subsequently quantified in PEAKS DB.

All the Orbitrap LTQ and MALDI-TOF/TOF mass spectrometry proteomics data have been deposited to the ProteomeXchange Consortium via the PRIDE[40] partner repository with the dataset identifier PXD006528 and 10.6019/PXD006528.

Ingenuity Pathway Analysis (IPA)

For pathway enrichment analysis of targeted and differentially regulated proteins, we used ingenuity software (http://www.ingenuity.com/). Chemoproteomic and differential expression data were imported with their UniProtKB accession numbers and log (fold change) values were imported. The IPA core analysis settings are shown in supplementary data IPA summary S-1.

Results

WA, but not WN, triggers apoptotic cell death in GC-resistant MM1R cells

WA-induced cell death has already been reported in many cancer cell types. Here, we further characterized WA-induced cell death in a glucocorticoid (GC)-resistant multiple myeloma (MM) cell model. Caspase-3 and PARP cleavage, two well-known markers of apoptotic cell death, were demonstrated by Western blot (figure 2). By varying the concentration and incubation times, we optimized treatment conditions for further proteomic experiments performed during the early stages of apoptosis. After 3 h of treatment with 1 µM WA, we could observe the events leading to cell death, which begins after 3 h (figure 2). Previous work by our research group on WA and MM1R cells determined an IC_{50} value of 1.5 µM WA.

Interestingly, the WA analog WN fails to trigger cell death, even at elevated concentrations (8 h treatment with 2 µM WN). Interestingly, dexamethasone also fails to induce cell death in MM1R cells, which consistent with the proposed model of GC therapy resistance in MM1R cells. The intriguing observation that WA, but not its analog WN, can overcome GC therapy resistance in MM1R cells prompted us to elucidate the molecular mechanism(s) leading towards WA-selective cell death. To this end, we applied a combination of quantitative shotgun proteomics, quantitative

chemoproteomics and subsequent protein expression data analysis using the strongly curated pathway analysis tool IPA (Ingenuity Pathway Analysis).

Differential proteomics-based identification of WA-regulated protein expression

Differential expression (shotgun) proteomic analysis was performed since multiple WA-dependent transcriptional changes may affect the expression levels of multiple WA-regulated proteins [8]. We selected WN treatment to be a negative control treatment since this compound has no tumor cytotoxic activity (figure 2), despite its structural similarity to WA (figure 1). In a competition experiment, we pretreated MM1R cells with various concentrations of WN for 30 min, followed by treatment with 0.5 µM WABI for 1 h 30 min and visualized target proteins using streptavidin HRP Western blot analysis (figure 3). Since the same bands where observed when cells were either pretreated or not pretreated with WN, we assume that no competition occurs between WN and WABI.

To characterize the effects of WA treatment on the dynamic changes in expression of the MM1R proteome, we differentially labeled MM1R cells with light and heavy lysine and arginine isotopes, and treated them for 3 h with WN and WA, respectively. Previous experiments revealed significant WA-specific protein expression changes as early as 3 h after treatment and at the onset of the tumor cytotoxic response, and it had minimal secondary effects [41]. After treatment and pooling of both proteomes, a 2D LC-MS/MS procedure was performed resulting in three possible SILAC ratio combinations (figure 4A). MALDI and ESI (Orbitrap) measurement data were combined to achieve the most sensitive analysis of WA-specific protein expression changes in the MM1R proteome.

MALDI TOF/TOF analysis resulted in 1015 unique proteins, of which 906 could be quantified (table S-1). Figure 5A shows the complete distribution, in which there were 42 WA-upregulated and 19 WA-downregulated proteins (all with ≥ 2-fold change). The same strategy was used with an Orbitrap mass spectrometer, resulting in 2512 proteins identified, of which 2005 could be quantified (table S-2). Again, plotting the complete proteome (figure 5B) demonstrated that WA differentially influences a

rather small set of proteins, as 121 upregulated and 79 downregulated proteins were identified and quantified (all with ≥ 2-fold change). Variations in absolute ratios are probably due to the use of different MS devices (MALDI vs. Orbitrap) and quantification software packages (ProteinPilot versus Peaks).Hence, when the quantification of proteins results in contradictory results between MALDI and Orbitrap, these proteins were excluded from the final list of denoted differentially expressed proteins upon WA treatment.

Upon the combination of the proteins identified using MALDI and Orbitrap mass spectrometry, we identified 90 upregulated and 53 downregulated proteins (table 1), with limited overlap between both methods, emphasizing the importance of using different ionization strategies.

WA-biotin-induced MM1R cell death depends on covalently bound cysteine-reactive target proteins

Next, we aimed at identifying the direct protein binding partners of WA via a biotin-labeled WA analog (WABI; figure 6A). Consistent with the structure-function studies of WA analogs, WABI showed no loss in antitumor activity, as observed by caspase-3 cleavage in MM1R cells (figure 6B) and as previously shown [12]. In a pilot experiment, we checked whether WABI treatment of MM1R cells resulted in specific WA-protein covalent binding. MM1R cells were treated with 1 µM WABI for 3 h, after which the WABI-bound proteins were enriched via streptavidin-biotin pull down. Eluting these target proteins with SDS-containing loading buffer and subsequent visualization by Western blot with streptavidin-HRP showed multiple WABI-targeted proteins in the MM1R proteome (figure 6C). The constitutive band corresponding to being approximately 95 kDa that was observed in both the input and the immunoprecipitated samples is probably an excessive endogenous biotinylated protein. In addition, since WA-protein binding most likely occurs via a Michael addition [42], the potential inhibitory effect of excessive amounts of the competitive nucleophilic thiol donor compound DTT was also tested. Results presented in figure 6C clearly show that when comparing the lysates from WABI - and WABI + DTT-treated cells, excess amounts of DTT (100 mM) react with the

electrophilic WABI molecule, leaving no functional groups that could additionally bind to the nucleophilic amino acids (e.g., cysteine) of target proteins present in the cell lysate.

Chemoproteomic characterization of WA-bound target proteins in MM1R cells

Since a large amount of WABI target proteins could be visualized after streptavidin-WABI pull down, we aimed to identify these proteins via 2D LC-MS/MS. The proteomes of WA- and WABI-treated MM1R cells were differentially labeled by growing the cells in media containing light ($^{12}C_6$) or heavy ($^{13}C_6$) isotope-labeled arginine and lysine (figure 4C). This labeling not only enabled us to discriminate between treatment conditions by means of the observed mass difference but also allowed for the detection of non-specific binding proteins, which did not have different abundances in the two conditions. Beads resulting from the streptavidin-WABI pulldown were directly digested with trypsin since elution of target proteins from the beads using different biochemical approaches proved unsatisfactory, which is a previously described phenomenon [43].

With this setup, any of three types of interactions were expected to occur, as shown in figure 4B. First, non-specific binding of proteins with the affinity matrix, denoted as NS in figure 4B. Since these identifications are not a result of the WABI treatment conditions, the intensities of the m/z peaks will be equal, as determined by the SILAC ratio (heavy/light SILAC ratio ≈ 1). Second, a specific interaction results in single peaks from heavy-or light-labeled peptides, denoted as S in figure 4B. A third type of identification differentiates between non-specific and specific interactions of WA-and WABI-treated MM1R cells (denoted as NS + S in figure 4B). These proteins non-specifically bind to the beads to some extent, yet they are also targeted by WABI, thereby increasing their abundance in the streptavidin pull down. Trinkle-Mulcahy *et al.* [44] were the first to combine SILAC ratios with pull-down experiments in this way, enabling researchers to account for these previously ignored potential targets.

A forward and reverse SILAC labeling strategy (figure 4C) was combined with MALDI-TOF/TOF mass spectrometry, which resulted in 809 and 842 protein identifications, respectively, and a total of 1041

unique proteins were identified. Of these uniquely identified proteins, 84 proteins were identified as being WA targets by the presence of exclusive single heavy (forward SILAC) or light (reverse SILAC) peptides in both measurements. Additionally, we quantified our chemoproteomic data to determine specific WA-protein interactions that are also non-specific (see above possibility 3). This experiment resulted in 9 additional WA protein targets (≥ 2 fold change, table S-4). A third chemoproteomics experiment was performed using an Orbitrap Velos LTQ mass spectrometer with WABI-and WA-treated MM1R cells labeled with heavy and light SILAC amino acids, respectively. This experiment resulted in 2426 unique protein identifications, of which 189 proteins were identified as being potential WABI targets based on single peak identifications. Additionally, we quantified the chemoproteomic data (table S-4), resulting in 83 proteins that had a heavy/light ratio of ≥ 2, suggesting that these proteins were also WABI targets.

Combining MALDI and Orbitrap chemoproteomic MS experiments resulted in 2581 unique protein identifications, including 208 potential WA target proteins (table S-4). An overview of the identified WA protein targets identified by both methods is shown in table 2.

Pathway analysis of WA-regulated proteins identifies selective cancer targets for treatment of monoclonal gammopathies, such as multiple myeloma and Waldenström macroglobulinemia

The above proteomics experiments underline the polypharmaceutical nature of WA, which may form the basis of its efficient antitumor effects. Unfortunately, from a pharmacotherapeutic point of view, multifunctionality is frequently associated with adverse side effects, making the current version of the WA molecule less attractive for further preclinical development. However, considering the various antitumor effects of WA, it might be possible to select the most effective pathways for more selective tumor targeting and drug optimization. Therefore, we introduced the 208 target proteins and the 143 differentially regulated proteins (table S-7) to the highly curated web-based IPA software (IPA summary S-1) and looked for enrichments in diseases and pathways.

By screening against “disease and function”, we further investigated the term ‘cancer’ (enrichment with a p-value between 1.11E-04-4.43E-02, figure 7A) since cancer has frequently shown to be disturbed by WA. From the 31 types of cancer described in IPA, enrichment was most prominent for Waldenström macroglobulinemia (WM, p-value = 3.00E-05) and plasma cell dyscrasia (p-value = 5.78E-04) (full list table S-5). Interestingly, plasma cell dyscrasia (p-value = 5.78E-04 and 20 unique proteins, figure 7B) is a collection of disorders related to the abnormal proliferation of monoclonal populations of plasma cells, denoted as monoclonal myeloma gammopathies. In addition to Waldenström macroglobulinemia and multiple myeloma, monoclonal gammopathy of undetermined significance (MGUS) are included. This finding indicates that many proteins identified in our proteomics studies are correlated with the biological cell model used (MM1R). Intriguingly, of the 20 unique cancer prone proteins assigned to plasma cell dyscrasia, WA reverses 16 tumor-promoting targets (table 3). For instance, heme oxygenase 1 (HMOX1), which is correlated with cellular stress [45], was shown to be strongly upregulated after WA treatment in both the 2D-LC-MALDI and 2D-LC-Orbitrap experiments (average 11.7-fold) and this result was confirmed by Western blot (figure 7C). Interestingly, HMOX1 is strongly downregulated in WM cells, as is shown by Hatjiharissi *et al.* [46], whereas our results show that WA reverses this process. Another protein we validated by Western blot was annexin A4 (ANXA4) (figure 7C), which is downregulated upon WA treatment according to the 2D-LC-Orbitrap experiment results (4.2-fold). In contrast, patients afflicted with WM and patients afflicted with MM typically promote upregulation of ANXA4, a protein important for exocytosis (secretion of antibodies) and motility (migrating cancer cells), by mending the plasma membrane after rupture [47]. Downregulation of this protein by WA may slow down this process, making the cancer cells more prone to lysis. We validated the upregulation of PSMB1. According to the 2D-LC-Orbitrap experiments, a two-fold upregulation was observed for this proteasome subunit in response to WA treatment compared to WN treatment in MM1R cells. Although semi-quantitative, Western blot likely confirms this result (figure 7C). Interestingly, a 2-4-fold upregulation of PSMB1 and PSMA2 expression has also been reported for treatment with bortezomib [48], a proteasome inhibitor used

as a clinical first-line therapy to treat both MM and WM, and this still resulted in cell death. Finally, streptavidin-biotin pull down and subsequent Western blot analysis showed binding of WA to the PSMB10 proteasome subunit, although this binding was limited (figure 7D). Thus, despite the described association of WA with the chymotrypsin-like catalytic proteasome subunit [49], our chemoproteomic approach and anti-PSMB10 Western blot validation suggest WA binding would impair the trypsin-like activity of the 20S proteasome.

WA influences the canonical pathways associated with protein ubiquitination

Next, we searched for matching biological pathways linked to the antitumor activity of WA (figure 8A). The protein ubiquitination pathway (-Log(p-value) = 3.13E00, figure S-1) was further investigated, as it is currently the main strategy for therapy against multiple myeloma in the clinic, with bortezomib (Velcade®) being the most representative compound. Of special note, WA has been shown to function as a proteasome inhibitor by inhibiting the chymotrypsin-like activity of proteasomes [26,27], and Western blot analysis with an anti-ubiquitin antibody confirmed a time- and concentration-dependent accumulation of ubiquitinated proteins (figure 8B). In addition, the WA-regulated proteins HLA-B, PSMB1, PSMA2 and PSMB10 that are associated with the ubiquitination pathway are also associated the plasma cell dyscrasia network (figure 7B), emphasizing the strong impact of WA on monoclonal myeloma gammopathies through inhibition of the ubiquitin-proteasome pathway.

Discussion

Tumors typically harbor cancer cells that have significant (epi)genetic heterogeneity, causing therapy relapse and the development of treatment resistance. Because of this, chemotherapy resistance is shifting the drug discovery paradigm from single-target to multi-target approaches. The steroidal lactone Withaferin A (WA) is such a promising antitumor drug, because it has multiple targets and potent antitumor properties. Despite these promising antitumor properties of WA, only fragmented

information about the underlying molecular mechanisms is available. Here, we provide the first global proteome-wide view of the WA antitumor effects on a GC-resistant multiple myeloma (MM1R) cell model. We SILAC labeled this MM1R cell line and characterized the direct and indirect antitumor effects of WA by using a quantitative shotgun strategy and a quantitative chemoproteomics approach.

For our differential expression analysis, we compared MM1R treatment of WA with its inactive analog WN. Based on two complementary measurements, we identified 143 differentially WA regulated proteins (all ≥ 2-fold change) of which 90 were upregulated and 53 were downregulated. Up until now, there has been only one differential proteomics study on WA action, performed by *Narayan et al.* [50] which identified 28 upregulated and 4 downregulated proteins in mouse N9 microglial cells after treatment with 2 µM WA for 24 h. An explanation for this lower number of WA-regulated proteins could be that Narayan *et al.* only used heavy-labeled lysine residues in their approach. Because of this, peptides cleaved at arginine residues were not included in the SILAC analysis, which subsequently lowered the score and number of identified and quantified proteins. Moreover, a different cell line and a different experimental workflow was used, which could also explain the different outcome. Nevertheless, some proteins showed similar trends in differential expression after WA treatment in both studies. For instance, both aldose reductase (ALDR), a cytosolic NADPH-dependent oxidoreductase that catalyzes the reduction of a variety of aldehydes and carbonyls (2.91-fold change in our study versus a 2.1-fold change by Narayan *et al.*) and heme oxygenase 1 (HMOX1, 11.7 versus 4.7) of which the expression is induced by oxidative stress, were upregulated in both studies. Additionally, both hematopoietic cell specific protein 1 (HCLS1, 2.23 versus 1.6), a prominent substrate of intracellular protein tyrosine kinases in hematopoietic cells, and peroxiredoxin-6 (PRDX6, 1.86 versus 1.8), a protein involved in the redox regulation of the cell, were upregulated. In contrast, annexin A4 (ANXA4), a calcium/phospholipid-binding protein that promotes membrane fusion and is involved in exocytosis, was found to be clearly downregulated in our

experiments according to MS (0.238-fold change) and Western blot analysis, while it was slightly upregulated (1.6-fold change) in the study by Narayan *et al*.. ANXA4 is upregulated in many different cancer models, including Waldenström macroglobulinemia, and consequently, a downregulation of this protein after treatment could be potentially therapeutic, which has already been described for flavonoids phytochemicals [51]. Once again, this finding notes that despite cell type-specific actions, a proteome-wide comparison of WA antitumor effects in various tumor cell types may be useful to identify a conserved antitumor mechanism across cell types. Of special note, GR-deficient MM1R cells are resistant to glucocorticoid (e.g., dexamethasone) treatment, and from our data it appears that WA elicits GC-like effects on these cancer cells (*Chirumamilla et al*., submitted). For instance, 3 of the top 15 upregulated proteins identified with the Orbitrap MS analysis (table 1) are also responsive to GC treatment: sepiapterin reductase (SPR), transcription elongation factor SPT6 (SUPT6H) and UTP-glucose-1-phosphate uridylyltransferase (UGP2). One interesting hypothesis that deserves further investigation is that WA might indirectly trigger GC-like effects, for example, by modulating the function of hsp90 function, which is a master regulator of hormone-receptor functions. Moreover, hsp90 inhibitors have been reported to restore GR function [52].

Our chemoproteomic approach required a biotin-labeled variant of WA (WABI), which showed no loss in antitumor activity (figure 2), to selectively enrich the direct WA-targeted proteins via streptavidin pull down. An on-bead digest with trypsin proved to be the best way to identify these enriched proteins. However, this approach can result in non-specific (false positive) protein identifications since a selection step is omitted [44]. Therefore, a SILAC labeling strategy was used to discriminate between specific and non-specific interactions, as previously reported [53]. This strategy resulted in the identification of 208 potential protein targets of WA based on 3 measurements.

Up until now, 15 WA target proteins have been described in the literature, with vimentin being the most well-known [9,16]. Unfortunately, in our study, vimentin displayed a high non-specific interaction, as determined by streptavidin pull down, and as already described for other types of

enrichment [53]. Nevertheless, when the chemoproteomic data were quantified, no differential ratio was observed for vimentin (ratio H/L = 0.99), indicating that this protein only binds non-specifically. The same is true for other described WA targets such as annexin A2 (ratio H/L = 1.02) [17,18] and β-tubulin (ratio H/L = 1.16) [19]. However, the binding of WA to β-tubulin is also accompanied by the downregulation of β-tubulin [19], as confirmed by our differential expression analysis. One possible explanation for this phenomenon is that the length of the spacer arm between WA and the biotin moiety could influence the chemoproteomics pull down. Additionally, WA targets may be cell type-specific. Cell culture systems like ours look at WA targets in living cells that have many different background molecules and structures. *In vitro* systems using only recombinant forms of the target proteins omit these problems, but move away from the actual biological mechanisms. Nonetheless, since deficiency models of vimentin, annexin A2 and β-tubulin do not completely abrogate the antitumor activity of WA, other relevant targets may contribute as well. We validated the binding of WA to PSMB10 via streptavidin pull down and Western blot with anti-PSMB10 antibody. So far the binding of WA to the chymotrypsin-like catalytic subunit of the proteasome has been described [54]. With PSMB10, a trypsin-like catalytic subunit, we propose another proteasome subunit is targeted by WA and results in the accumulation of ubiquitinated proteins.

Combining both proteomics experiments with Ingenuity Pathway Analysis (IPA) resulted in the identification of WA-selective protein networks that are highly involved in plasma cell dyscrasia (PCD) diseases, such as multiple myeloma and Waldenström macroglobulinemia. Assuming that binding of WA impairs protein function, WA reverses the effect 16 of the 20 PCD-associated proteins assigned by IPA, suggesting WA could counteract the disease progression of PCD.

The plasma cells associated with the PCD diseases have the distinct ability to secrete antibodies and therefore are committed to massive Ig synthesis, assembly and secretion. Due to this, plasma cells undergo substantial endoplasmic and oxidative stresses [55]. Moreover, the oncogenic transformation of plasma cells results in even higher protein synthesis rates ultimately leading to exacerbation of the ER stress and oxidative stress [56]. These stresses indicate a crucial role for the

proteasome, since this protein complex ensures degradation of wrongly translated or misfolded proteins as a consequence of the higher protein synthesis rate during oncogenic transformation. Interestingly, the PCD-associated network contains three proteasome subunits: PSMB10, PSMB1 and PSMA2 and additional pathway analysis showed that WA has a major impact on the protein ubiquitination pathway (figure 8). Our chemoproteomic studies reveal that WA is a proteasome inhibitor [27,49] through its binding with the PSMB10 proteasome subunit as suggested by the accumulation of ubiquitinated proteins (figure 8). The upregulation of both the PSMB1 and PSMA2 subunit is probably a consequence of the proteasome homeostasis mechanism, trying to restore proteasomal function [57,58]. Indeed, proteasome inhibition results in upregulation of nearly every proteasome subunit, leading to the *de novo* assembly of complete new proteasomes [59]. This is observed after short term treatment with proteasome inhibitors and it looks like WA induces the same effect after 3 hours of treatment. Two NF-E2-related transcription factors (Nrf1 and Nrf2) play a central role in the regulation of the proteasome genes and the type of stress will determine which pathway will be used. Proteotoxic stress as a result of proteasome inhibition will result in proteasome gene upregulation via the Nrf1 transcription factor [60] (figure 9). On the other hand, the Nrf2 transcription factor induces proteasome gene transcription during oxidative stress [59], which is also induced by WA (see below). Thus from our PCD network we hypothesize that WA can act on both pathways, thereby underlining its multifunctional antitumor nature.

Besides ubiquitin-proteasome mediated protein degradation, the lysosomal macro-autophagy pathway is also involved in the constitutive turnover of proteins, cytoplasm and whole organelles, thereby serving as a protective cellular response [61] (figure 9). Diverse cellular stresses like protein aggregation can increase its activity rapidly. The autophagosomes from cells under different conditions, for instance starvation, revealed two classes of proteins: those that always appear to associate with autophagosomes and those that appear to associate with autophagosomes in a cell condition-dependent manner [62]. Interestingly, different research groups have already described the WA impaired autophagy in different cancer cell types [63–65], but the underlying molecular

interactors remain unknown. From our PCD network, we identified HDAC6 and ANXA4 as autophagy associated proteins targeted by WA [62,66]. As a result of the WA induced downregulation of ANXA4, the membrane formation, essential for autophagosome vesicle docking and fusion with the lysosome, is probably impaired [62]. Due to the binding of WA with HDAC6, autophagosome formation may also be impaired since HDAC6 controls the fusion of autophagosomes to lysosomes [67]. Combination therapies with HDAC6 inhibitors, bortezomib and dexamethasone are nowadays used against MM [68] and since WA has been shown to partially mimic glucocorticoid receptor activation (*Chirumamilla et al*., submitted, see above) this one molecule seems to combine the strengths of each therapy. The above described WA targets are therefore of great promise for further research and further studies are needed to understand WA dependent cargo recruitment to autophagosomes.

Although not associated with the PCD network, it is noteworthy to further validate the binding of WA with the heat shock factor 1 (HSF1). HSF1 responds to proteotoxic stress, e.g. after proteasome inhibition by bortezomib [69,70], by upregulation of the heat shock proteins. Interestingly, HSF1 is highly upregulated in MM where it is considered as a potential new therapeutic antitumor target [71]. Moreover, the HSF1 stress response pathway also regulates autophagy [72], suggesting a central role for HSF1 in cellular stress response (figure 9). Interestingly, it has been described that simultaneous inhibition of the ubiquitin-proteasome system and autophagy by WA enhances apoptosis in human pancreatic cancer cells [65]. Our data confirm these results in MM cells and provide further molecular evidence for this hypothesis.

Our differential expression analysis showed an upregulation of the heme oxygenase 1 (HMOX1) protein which is downstream in the Nrf2 pathway. This suggests WA induces oxidative stress upon which MM cells compensate by upregulation of the proteasome genes via the Nrf2 transcription factor [41] (figure 9). Indeed, oxidative stress has already been associated with WA treatment [20,22], possibly because of its electrophilic characteristics which enables the molecule to bind covalently to cysteine-containing redox-sensing proteins like KEAP1 [41]. Nowadays, electrophilic

compounds, like WA, are extensively studied for their redox regulation of antioxidants, autophagy, and the response to stress for their application in so-called electrophile therapeutics [73]. Although presented as two independent pathways, both proteotoxic and oxidative stress have been described intertwined. For instance, proteasome inhibition results in accumulation of unfolded proteins and triggers endoplasmic reticulum (ER) stress [74]. If unresolved, this ER stress has been shown to cause cell death via multiple pathways in MM, including overproduction of reactive oxygen species (ROS) [74]. Interestingly, ROS generation has been shown to precede the initiation of bortezomib induced apoptosis [75] and co-treatment with the antioxidant tiron could largely undo this bortezomib-induced ROS generation and cell death [76]. The same was observed for WA treated HCT 116 cells that where pretreated with ROS scavenger N-acetyl-L-cysteine (NAC) which ablated the antitumor effect of WA [77]. This means that WA-induced oxidative stress could be the result of both its electrophilic and its proteasome-inhibitory activity. While WA may also exert other antitumor mechanisms like kinase inhibition [78] or NF-kB inhibition [12], our data show that WA puts a massive pressure on several arms of the protein degradation pathways while at the same time increases oxidative stress. Therefore, by firmly closing the proteotoxic and oxidative stress pathways that enable cancer cells to cope with high amounts of stress, the rapid and strong antitumor effect of WA towards MM cells and PCD could be explained.

In conclusion, we believe that by combining differential proteomic expression analysis of WA-treated MM1R cells and chemoproteomic identification of WA-interacting proteins, it becomes possible to resolve cancer-specific (chemosensitization) pathways influenced by WA. Dissection of the molecular mechanism of a strong antitumor compound like WA may pave the way towards the development of new drugs or more specific WA analogs with improved druggability, efficacy and selectivity, to be used in preclinical research.

References

[1] P. Borst, Cancer drug pan-resistance: pumps, cancer stem cells, quiescence, epithelial to mesenchymal transition, blocked cell death pathways, persisters or what?, Open Biol. 2 (2012) 120066–120066. doi:10.1098/rsob.120066.

[2] R.H. Wijdeven, B. Pang, Y.G. Assaraf, J. Neefjes, Old drugs, novel ways out: Drug resistance toward cytotoxic chemotherapeutics, Drug Resist. Updat. 28 (2016) 65–81. doi:10.1016/j.drup.2016.07.001.

[3] S. de Mel, S.H. Lim, M.L. Tung, W. Chng, Implications of Heterogeneity in Multiple Myeloma, Biomed Res. Int. 2014 (2014) 12. doi:10.1155/2014/232546.

[4] F. Schmidt, T. Efferth, Tumor heterogeneity, single-cell sequencing, and drug resistance, Pharmaceuticals. 9 (2016). doi:10.3390/ph9020033.

[5] J.L. Medina-Franco, M.A. Giulianotti, G.S. Welmaker, R.A. Houghten, Shifting from the single to the multitarget paradigm in drug discovery, Drug Discov. Today. 18 (2013) 495–501. doi:10.1016/j.drudis.2013.01.008.

[6] D. Hanahan, R. a. Weinberg, Hallmarks of cancer: The next generation, Cell. 144 (2011) 646–674. doi:10.1016/j.cell.2011.02.013.

[7] I.-C. Lee, B. Choi, Withaferin-A—A Natural Anticancer Agent with Pleitropic Mechanisms of Action, Int. J. Mol. Sci. 17 (2016) 290. doi:10.3390/ijms17030290.

[8] K. Szarc Vel Szic, K. Op De Beeck, D. Ratman, A. Wouters, I.M. Beck, K. Declerck, K. Heyninck, E. Fransen, M. Bracke, K. De Bosscher, F. Lardon, G. Van Camp, W. Vanden Berghe, Pharmacological levels of Withaferin A (Withania somnifera) trigger clinically relevant anticancer effects specific to triple negative breast cancer cells, PLoS One. 9 (2014). doi:10.1371/journal.pone.0087850.

[9] P. Bargagna-Mohan, A. Hamza, Y.E. Kim, Y. Khuan (Abby) Ho, N. Mor-Vaknin, N. Wendschlag, J. Liu, R.M. Evans, D.M. Markovitz, C.G. Zhan, K.B. Kim, R. Mohan, The Tumor Inhibitor and Antiangiogenic Agent Withaferin A Targets the Intermediate Filament Protein Vimentin, Chem. Biol. 14 (2007) 623–634. doi:10.1016/j.chembiol.2007.04.010.

[10] S. Saha, M. Islam, J. a Shilpi, S. Hasan, Inhibition of VEGF: a novel mechanism to control angiogenesis by Withania somnifera's key metabolite Withaferin A, Silico Pharmacol. 1 (2013) 11. doi:10.1186/2193-9616-1-11.

[11] S. Ashkenazi, A. Plotnikov, A. Bahat, E. Ben-Zeev, S. Warszawski, R. Dikstein, A Novel Allosteric Mechanism of NF-κB Dimerization and DNA Binding Targeted by an Anti-Inflammatory Drug., Mol. Cell. Biol. 36 (2016) 1237–47. doi:10.1128/MCB.00895-15.

[12] K. Heyninck, M. Lahtela-kakkonen, P. Van Der Veken, G. Haegeman, W. Vanden, Withaferin A inhibits NF-kappaB activation by targeting cysteine 179 in IKK b, Biochem. Pharmacol. (2014). doi:10.1016/j.bcp.2014.08.004.

[13] T.Z. Lv, G.S. Wang, Antiproliferation potential of withaferin A on human osteosarcoma cells via the inhibition of G2 / M checkpoint proteins, (2015) 323–329. doi:10.3892/etm.2015.2480.

[14] W. Suttana, S. Mankhetkorn, W. Poompimon, A. Palagani, S. Zhokhov, S. Gerlo, G. Haegeman, W. Vanden Berghe, Differential chemosensitization of P-glycoprotein overexpressing K562/Adr cells by withaferin A and Siamois polyphenols., Mol. Cancer. 9 (2010) 99. doi:10.1186/1476-4598-9-99.

[15] P. Joshi, L. Misra, A.A. Siddique, M. Srivastava, S. Kumar, M.P. Darokar, Epoxide group relationship with cytotoxicity in withanolide derivatives from Withania somnifera, Steroids. 79 (2014) 19–27. doi:10.1016/j.steroids.2013.10.008.

[16] G. Lahat, Q.S. Zhu, K.L. Huang, S. Wang, S. Bolshakov, J. Liu, K. Torres, R.R. Langley, A.J. Lazar, M.C. Hung, D. Lev, Vimentin is a novel anti-cancer therapeutic target; insights from In Vitro

and In Vivo mice xenograft studies, PLoS One. 5 (2010). doi:10.1371/journal.pone.0010105.

[17] R.R. Falsey, M.T. Marron, G.M.K.B. Gunaherath, N. Shirahatti, D. Mahadevan, a a L. Gunatilaka, L. Whitesell, Actin microfilament aggregation induced by withaferin A is mediated by annexin II., Nat. Chem. Biol. 2 (2006) 33–8. doi:10.1038/nchembio755.

[18] G. Ozorowski, C.M. Ryan, J.P. Whitelegge, H. Luecke, Withaferin A binds covalently to the N-terminal domain of annexin A2, Biol. Chem. 393 (2012) 1151–1163. doi:10.1515/hsz-2012-0184.

[19] M.L. Antony, J. Lee, E.R. Hahm, S.H. Kim, A.I. Marcus, V. Kumari, X. Ji, Z. Yang, C.L. Vowell, P. Wipf, G.T. Uechi, N. a. Yates, G. Romero, S.N. Sarkar, S. V. Singh, Growth arrest by the antitumor steroidal lactone withaferin a in human breast cancer cells is associated with down-regulation and covalent binding at cysteine 303 of β-tubulin, J. Biol. Chem. 289 (2014) 1852–1865. doi:10.1074/jbc.M113.496844.

[20] F. Malik, A. Kumar, S. Bhushan, S. Khan, A. Bhatia, K.A. Suri, G.N. Qazi, J. Singh, Reactive oxygen species generation and mitochondrial dysfunction in the apoptotic cell death of human myeloid leukemia HL-60 cells by a dietary compound withaferin A with concomitant protection by N-acetyl cysteine, Apoptosis. 12 (2007) 2115–2133. doi:10.1007/s10495-007-0129-x.

[21] E. Mayola, C. Gallerne, D.D. Esposti, C. Martel, S. Pervaiz, L. Larue, B. Debuire, A. Lemoine, C. Brenner, C. Lemaire, Withaferin A induces apoptosis in human melanoma cells through generation of reactive oxygen species and down-regulation of Bcl-2., Withaferin A Induces Apoptosis Hum. Melanoma Cells through Gener. React. Oxyg. Species down-Regulation Bcl-2. 16 (2011) 1014–1027. doi:10.1007/s10495-011-0625-x.

[22] S.M. Yu, S.J. Kim, Production of reactive oxygen species by withaferin A causes loss of type collagen expression and COX-2 expression through the PI3K/Akt, p38, and JNK pathways in

rabbit articular chondrocytes, Exp. Cell Res. 319 (2013) 2822–2834. doi:10.1016/j.yexcr.2013.08.026.

[23] S. Srinivasan, R.S. Ranga, R. Burikhanov, S.S. Han, D. Chendil, Par-4-dependent apoptosis by the dietary compound withaferin A in prostate cancer cells, Cancer Res. 67 (2007) 246–253. doi:10.1158/0008-5472.CAN-06-2430.

[24] H. Amin, D. Nayak, R. ur Rasool, S. Chakraborty, A. Kumar, K. Yousuf, P.R. Sharma, Z. Ahmed, N. Sharma, A. Magotra, D. Mukherjee, L.D. Kumar, A. Goswami, Par-4 dependent modulation of cellular ??-catenin by medicinal plant natural product derivative 3-azido Withaferin A, Mol. Carcinog. 55 (2016) 864–881. doi:10.1002/mc.22328.

[25] B. Rah, H. Amin, K. Yousuf, S. Khan, G. Jamwal, D. Mukherjee, A. Goswami, A Novel MMP-2 Inhibitor 3-azidowithaferin A (3-azidoWA) Abrogates Cancer Cell Invasion and Angiogenesis by Modulating Extracellular Par-4, PLoS One. 7 (2012). doi:10.1371/journal.pone.0044039.

[26] H. Yang, G. Shi, Q.P. Dou, The tumor proteasome is a primary target for the natural anticancer compound Withaferin A isolated from “Indian winter cherry”., Mol. Pharmacol. 71 (2007) 426–437. doi:10.1124/mol.106.030015.

[27] S. Khan, A.W. Rammeloo, J.J. Heikkila, Withaferin A Induces Proteasome Inhibition, Endoplasmic Reticulum Stress, the Heat Shock Response and Acquisition of Thermotolerance, PLoS One. 7 (2012). doi:10.1371/journal.pone.0050547.

[28] S.S. Jackson, C. Oberley, C.P. Hooper, K. Grindle, S. Wuerzberger-davis, J. Wolff, K. Mccool, L. Rui, S. Miyamoto, Withaferin A disrupts ubiquitin-based NEMO reorganization induced by canonical NF- κ B signaling, Exp. Cell Res. (2014). doi:10.1016/j.yexcr.2014.09.034.

[29] L.P. Yco;, G. Mocz;, J. Opuku-Ansah, A.S. Bachmann, W.A. Inhibits, I. Tumor, C. Death, Withaferin A Inhibits STAT3 and Induces Tumor Cell Death in Neuroblastoma and Multiple Myeloma, Biochem. Insights. 7 (2014) 1–13. doi:10.4137/BCI.S18863.

[30] E.-R. Hahm, J. Lee, S.-H. Kim, A. Sehrawat, J. a Arlotti, S.S. Shiva, R. Bhargava, S. V Singh, Metabolic alterations in mammary cancer prevention by withaferin A in a clinically relevant mouse model., J. Natl. Cancer Inst. 105 (2013) 1111–22. doi:10.1093/jnci/djt153.

[31] A.R. Vyas, S. V Singh, Molecular targets and mechanisms of cancer prevention and treatment by withaferin a, a naturally occurring steroidal lactone., AAPS J. 16 (2014) 1–10. doi:10.1208/s12248-013-9531-1.

[32] R. a. Kyle, S.V. Rajkumar, ASH 50th anniversary review, Blood. 111 (2008) 2962–2972. doi:10.1182/blood-2007-08-078139.

[33] T. Melarangi, J. Zhuang, K. Lin, N. Rockliffe, A.G. Bosanquet, M. Oates, J.R. Slupsky, A.R. Pettitt, Glucocorticoid resistance in chronic lymphocytic leukaemia is associated with a failure of upregulated Bim/Bcl-2 complexes to activate Bax and Bak, Cell Death Dis. 16 (2012) e372. doi:10.1038/cddis.2012.102.

[34] M. Vaiou, E. Pangou, P. Liakos, N. Sakellaridis, G. Vassilopoulos, K. Dimas, C. Papandreou, Endothelin-1 (ET-1) induces resistance to bortezomib in human multiple myeloma cells via a pathway involving the ETB receptor and upregulation of proteasomal activity, J. Cancer Res. Clin. Oncol. 142 (2016) 1–18. doi:10.1007/s00432-016-2216-2.

[35] D. Dytfeld, M. Luczak, T. Wrobel, L. Usnarska-, A. Nowicki, M. Joks, E. Czechowska, Comparative proteomic profiling of refractory / relapsed multiple myeloma reveals biomarkers involved in resistance to bortezomib-based therapy, Oncotarget. 7 (2016). doi:10.18632/oncotarget.11059.

[36] N. Malara, D. Focà, F. Casadonte, M.F. Sesto, L. Macrina, L. Santoro, M. Scaramuzzino, R. Terracciano, R. Savino, Simultaneous inhibition of the constitutively activated nuclear factor κB and of the Interleukin-6 pathways is necessary and sufficient to completely overcome apoptosis resistance of human U266 myeloma cells, Cell Cycle. 7 (2014) 3235–3245.

doi:10.4161/cc.7.20.6832.

[37] G.A.A. Van Raemdonck, W.A.A. Tjalma, E.P. Coen, C.E. Depuydt, X.W.M. Van Ostade, Identification of protein biomarkers for cervical cancer using human cervicovaginal fluid, PLoS One. 9 (2014). doi:10.1371/journal.pone.0106488.

[38] J.E. Elias, W. Haas, B.K. Faherty, S.P. Gygi, Comparative evaluation of mass spectrometry platforms used in large-scale proteomics investigations., Nat Methods. 2 (2005) 667–675. doi:10.1038/nmeth785.

[39] W.H. Tang, I. V. Shilov, S.L. Seymour, Nonlinear fitting method for determining local false discovery rates from decoy database searches, J. Proteome Res. 7 (2008) 3661–3667. doi:10.1021/pr070492f.

[40] J.A. Vizcaino, A. Csordas, N. Del-Toro, J.A. Dianes, J. Griss, I. Lavidas, G. Mayer, Y. Perez-Riverol, F. Reisinger, T. Ternent, Q.W. Xu, R. Wang, H. Hermjakob, 2016 update of the PRIDE database and its related tools, Nucleic Acids Res. 44 (2016) D447–D456. doi:10.1093/nar/gkv1145.

[41] K. Heyninck, L. Sabbe, C.S. Chirumamilla, K. Szarc Vel Szic, P. Vander Veken, K.J.A. Lemmens, M. Lahtela-Kakkonen, S. Naulaerts, K. Op De Beeck, K. Laukens, G. Van Camp, A.R. Weseler, A. Bast, G.R.M.M. Haenen, G. Haegeman, W. Vanden Berghe, Withaferin A induces heme oxygenase (HO-1) expression in endothelial cells via activation of the Keap1/Nrf2 pathway, Biochem. Pharmacol. 109 (2016) 48–61. doi:10.1016/j.bcp.2016.03.026.

[42] L. Misra, P. Lal, N.D. Chaurasia, R.S. Sangwan, S. Sinha, R. Tuli, Selective reactivity of 2-mercaptoethanol with 5??,6??-epoxide in steroids from Withania somnifera, Steroids. 73 (2008) 245–251. doi:10.1016/j.steroids.2007.10.006.

[43] H. Fukuyama, S. Ndiaye, J. Hoffmann, J. Rossier, S. Liuu, J. Vinh, Y. Verdier, On-bead tryptic proteolysis: An attractive procedure for LC-MS/MS analysis of the Drosophila caspase 8

protein complex during immune response against bacteria, J. Proteomics. 75 (2012) 4610–4619. doi:10.1016/j.jprot.2012.03.003.

[44] L. Trinkle-Mulcahy, S. Boulon, Y.W. Lam, R. Urcia, F.M. Boisvert, F. Vandermoere, N. a. Morrice, S. Swift, U. Rothbauer, H. Leonhardt, A. Lamond, Identifying specific protein interaction partners using quantitative mass spectrometry and bead proteomes, J. Cell Biol. 183 (2008) 223–239. doi:10.1083/jcb.200805092.

[45] R. Gozzelino, V. Jeney, M.P. Soares, Mechanisms of cell protection by heme oxygenase-1., Annu. Rev. Pharmacol. Toxicol. 50 (2010) 323–354. doi:10.1146/annurev.pharmtox.010909.105600.

[46] E. Hatjiharissi, H. Ngo, A.A. Leontovich, X. Leleu, M. Timm, M. Melhem, D. George, G. Lu, J. Ghobrial, Y. Alsayed, S. Zeismer, M. Cabanela, A. Nehme, X. Jia, A.S. Moreau, S.P. Treon, R. Fonseca, M.A. Gertz, K.C. Anderson, T.E. Witzig, I.M. Ghobrial, Proteomic analysis of Waldenstrom macroglobulinemia, Cancer Res. 67 (2007) 3777–3784. doi:10.1158/0008-5472.CAN-06-3089.

[47] C. Protzel, M. Richter, M. Poetsch, C. Kakies, U. Zimmermann, C. Woenckhaus, K.J. Klebingat, O.W. Hakenberg, J. Giebel, The role of annexins I, II and IV in tumor development, progression and metastasis of human penile squamous cell carcinomas, World J. Urol. 29 (2011) 393–398. doi:10.1007/s00345-010-0575-x.

[48] J.S. Gelman, J. Sironi, I. Berezniuk, S. Dasgupta, L.M. Castro, F.C. Gozzo, E.S. Ferro, L.D. Fricker, Alterations of the Intracellular Peptidome in Response to the Proteasome Inhibitor Bortezomib, PLoS One. 8 (2013). doi:10.1371/journal.pone.0053263.

[49] H. Yang, G. Shi, Q.P. Dou, The tumor proteasome is a primary target for the natural anticancer compound Withaferin A isolated from “Indian winter cherry”., Mol. Pharmacol. 71 (2007) 426–437. doi:10.1124/mol.106.030015.

[50] M. Narayan, K.W. Seeley, U.K. Jinwal, Identification and quantitative analysis of cellular proteins affected by treatment with withaferin a using a SILAC-based proteomics approach, J. Ethnopharmacol. 175 (2015) 86–92. doi:10.1016/j.jep.2015.09.024.

[51] A.K. Nagappan, V. Venkatarame, G. Saralamma, G.E. Hong, H.J. Lee, S.C. Shin, E.H. Kim, W.S. Lee, G.S. Kim, Proteomic analysis of selective cytotoxic anticancer properties of flavonoids isolated from Citrus platymamma on A549 human lung cancer cells, Mol. Med. Rep. 14 (2016) 3814–3822. doi:10.3892/mmr.2016.5666.

[52] G.K.S.& M.P.-P. Riebold Mathias, Christian Kozany, Lee Freiburger, Michael Sattler, Michael Buchfelder, Felix Hausch, A C-terminal HSP90 inhibitor restores glucocorticoid sensitivity and relieves a mouse allograft model of Cushing disease, Nat. Med. 21 (2015) 276–280. doi:10.1038/nm.3776.

[53] L. Trinkle-Mulcahy, S. Boulon, Y.W. Lam, R. Urcia, F.M. Boisvert, F. Vandermoere, N.A. Morrice, S. Swift, U. Rothbauer, H. Leonhardt, A. Lamond, Identifying specific protein interaction partners using quantitative mass spectrometry and bead proteomes, J. Cell Biol. 183 (2008) 223–239. doi:10.1083/jcb.200805092.

[54] H. Yang, Y. Wang, V.T. Cheryan, W. Wu, C.Q. Cui, L.A. Polin, H.I. Pass, Q.P. Dou, A.K. Rishi, A. Wali, Withaferin a inhibits the proteasome activity in mesothelioma in vitro and in vivo, PLoS One. 7 (2012) 14–16. doi:10.1371/journal.pone.0041214.

[55] S. Masciarelli, R. Sitia, Building and operating an antibody factory: Redox control during B to plasma cell terminal differentiation, Biochim. Biophys. Acta - Mol. Cell Res. 1783 (2008) 578–588. doi:10.1016/j.bbamcr.2008.01.003.

[56] S. White-Gilbertson, Y. Hua, B. Liu, The role of endoplasmic reticulum stress in maintaining and targeting multiple myeloma: A double-edged sword of adaptation and apoptosis, Front. Genet. 4 (2013) 1–8. doi:10.3389/fgene.2013.00109.

[57] Z. Sha, A.L. Goldberg, Proteasome-mediated processing of Nrf1 is essential for coordinate induction of all proteasome subunits and p97, Curr. Biol. 24 (2014) 1573–1583. doi:10.1016/j.cub.2014.06.004.

[58] A.M. Pickering, R.A. Linder, H. Zhang, H.J. Forman, K.J.A. Davies, Nrf2-dependent induction of proteasome and Pa28αβ regulator are required for adaptation to oxidative stress, J. Biol. Chem. 287 (2012) 10021–10031. doi:10.1074/jbc.M111.277145.

[59] M.-K. Kwak, N. Wakabayashi, J.L. Greenlaw, M. Yamamoto, T.W. Kensler, Antioxidants Enhance Mammalian Proteasome Expression through the Keap1-Nrf2 Signaling Pathway, Mol. Cell. Biol. 23 (2003) 8786–8794. doi:10.1128/MCB.23.23.8786-8794.2003.

[60] S.K. Radhakrishnan, C.S. Lee, P. Young, A. Beskow, J.Y. Chan, R.J. Deshaies, Transcription Factor Nrf1 Mediates the Proteasome Recovery Pathway after Proteasome Inhibition in Mammalian Cells, Mol. Cell. 38 (2010) 17–28. doi:10.1016/j.molcel.2010.02.029.

[61] N. Mizushima, B. Levine, A.M. Cuervo, D.J. Klionsky, Autophagy fights disease through cellular self-digestion, Nature. 451 (2008) 1069–1075. doi:10.1038/nature06639.

[62] J. Dengjel, M. Hoyer-Hansen, M.O. Nielsen, T. Eisenberg, L.M. Harder, S. Schandorff, T. Farkas, T. Kirkegaard, A.C. Becker, S. Schroeder, K. Vanselow, E. Lundberg, M.M. Nielsen, A.R. Kristensen, V. Akimov, J. Bunkenborg, F. Madeo, M. Jaattela, J.S. Andersen, Identification of Autophagosome-associated Proteins and Regulators by Quantitative Proteomic Analysis and Genetic Screens, Mol. Cell. Proteomics. 11 (2012) M111.014035-M111.014035. doi:10.1074/mcp.M111.014035.

[63] Y. Nishikawa, D. Okuzaki, K. Fukushima, S. Mukai, S. Ohno, Y. Ozaki, N. Yabuta, H. Nojima, Withaferin A induces cell death selectively in androgen-independent prostate cancer cells but not in normal fibroblast cells, PLoS One. 10 (2015) 1–20. doi:10.1371/journal.pone.0134137.

[64] E.-R. Hahm, S. V Singh, Autophagy fails to alter withaferin A-mediated lethality in human

breast cancer cells., Curr. Cancer Drug Targets. 13 (2013) 640–650.

[65] X. Li, F. Zhu, J. Jiang, C. Sun, Q. Zhong, M. Shen, X. Wang, R. Tian, C. Shi, M. Xu, F. Peng, X. Guo, J. Hu, D. Ye, M. Wang, R. Qin, Simultaneous inhibition of the ubiquitin-proteasome system and autophagy enhances apoptosis induced by ER stress aggravators in human pancreatic cancer cells, Autophagy. 12 (2016) 1521–1537. doi:10.1080/15548627.2016.1191722.

[66] T. Hideshima, J. Qi, R.M. Paranal, W. Tang, E. Greenberg, N. West, M.E. Colling, G. Estiu, R. Mazitschek, J.A. Perry, H. Ohguchi, F. Cottini, N. Mimura, G. Görgün, Y.-T. Tai, P.G. Richardson, R.D. Carrasco, O. Wiest, S.L. Schreiber, K.C. Anderson, J.E. Bradner, Discovery of selective small-molecule HDAC6 inhibitor for overcoming proteasome inhibitor resistance in multiple myeloma, Proc. Natl. Acad. Sci. 113 (2016) 13162–13167. doi:10.1073/pnas.1608067113.

[67] J.-Y. Lee, H. Koga, Y. Kawaguchi, W. Tang, E. Wong, Y.-S. Gao, U.B. Pandey, S. Kaushik, E. Tresse, J. Lu, J.P. Taylor, A.M. Cuervo, T.-P. Yao, HDAC6 controls autophagosome maturation essential for ubiquitin-selective quality-control autophagy., EMBO J. 29 (2010) 969–80. doi:10.1038/emboj.2009.405.

[68] D.T. Vogl, N. Raje, S. Jagannath, P. Richardson, P. Hari, R. Orlowski, J.G. Supko, D. Tamang, M. Yang, S.S. Jones, C. Wheeler, R.J. Markelewicz, S. Lonial, Ricolinostat, the First Selective Histone Deacetylase 6 Inhibitor, in Combination with Bortezomib and Dexamethasone for Relapsed or Refractory Multiple Myeloma., 2017. doi:10.1158/1078-0432.CCR-16-2526.

[69] S.P. Shah, A.K. Nooka, D.L. Jaye, N.J. Bahlis, S. Lonial, L.H. Boise, Bortezomib-induced heat shock response protects multiple myeloma cells and is activated by heat shock factor 1 serine 326 phosphorylation, Oncotarget. 5 (2016) 59727–59741. doi:10.18632/oncotarget.10847.

[70] J. Anckar, L. Sistonen, Regulation of HSF1 function in the heat stress response: implications in aging and disease., Annu. Rev. Biochem. 80 (2011) 1089–1115. doi:10.1146/annurev-biochem-060809-095203.

[71] T. Heimberger, M. Andrulis, S. Riedel, T. St??hmer, H. Schraud, A. Beilhack, T. Bumm, B. Bogen, H. Einsele, R.C. Bargou, M. Chatterjee, The heat shock transcription factor 1 as a potential new therapeutic target in multiple myeloma, Br. J. Haematol. 160 (2013) 465–476. doi:10.1111/bjh.12164.

[72] Y. Watanabe, A. Tsujimura, K. Taguchi, HSF1 stress response pathway regulates autophagy receptor SQSTM1 / p62-associated proteostasis, 8627 (2017) 133–148. doi:10.1080/15548627.2016.1248018.

[73] A.L. Levonen, B.G. Hill, E. Kansanen, J. Zhang, V.M. Darley-Usmar, Redox regulation of antioxidants, autophagy, and the response to stress: Implications for electrophile therapeutics, Free Radic. Biol. Med. 71 (2014) 196–207. doi:10.1016/j.freeradbiomed.2014.03.025.

[74] E.A. Obeng, L.M. Carlson, D.M. Gutman, W.J.H. Jr, K.P. Lee, L.H. Boise, Proteasome inhibitors induce a terminal unfolded protein response in multiple myeloma cells, Blood. 107 (2006) 4907–4917. doi:10.1182/blood-2005-08-3531.Supported.

[75] P. Pérez-Galán, G. Roue, N. Villamor, E. Montserrat, E. Campo, D. Colomer, The proteasome inhibitor bortezomib induces apoptosis in mantle-cell lymphoma through generation of ROS and Noxa activation independent of p53 status, Blood. 107 (2006) 257–264. doi:10.1182/blood-2005-05-2091.

[76] D. Llobet, N. Eritja, M. Encinas, A. Sorolla, A. Yeramian, J.A. Schoenenberger, A. Llombart-Cussac, R.M. Marti, X. Matias-Guiu, X. Dolcet, Antioxidants block proteasome inhibitor function in endometrial carcinoma cells., Anticancer. Drugs. 19 (2008) 115–124. doi:10.1097/CAD.0b013e3282f24031.

[77] a Kostecka, a Sznarkowska, K. Meller, P. Acedo, Y. Shi, H. a Mohammad Sakil, a Kawiak, M. Lion, a Królicka, M. Wilhelm, a Inga, J. Zawacka-Pankau, JNK-NQO1 axis drives TAp73-

mediated tumor suppression upon oxidative and proteasomal stress., Cell Death Dis. 5 (2014) e1484. doi:10.1038/cddis.2014.408.

[78] C.S. Chirumamilla, C. Pérez-Novo, X. Van Ostade, W. Vanden Berghe, Molecular insights into cancer therapeutic effects of the dietary medicinal phytochemical withaferin A, Proc. Nutr. Soc. (2017) 1–10. doi:10.1017/S0029665116002937.

Tables

Table 1: Top 15 differentially upregulated (≥ 2-fold) and downregulated (≥ 2-fold) proteins identified by MALDI TOF/TOF and Orbitrap MS/MS analysis. A complete list of all differentially regulated proteins (≥ 2-fold change) can be found in the supplementary table S-3.

Protein Name	UniProtKB Entry	UniProtKB Entry Name	Fold change	Standard Deviation
Upregulated ≥2 fold				
Sepiapterin reductase	P35270	SPRE_HUMAN	52.827	
RNA 3'-terminal phosphate cyclase-like protein	Q9Y2P8	RCL1_HUMAN	25.86	
Cation-independent mannose-6-phosphate receptor	P11717	MPRI_HUMAN	24.01	
Transmembrane emp24 domain-containing protein 2	Q15363	TMED2_HUMAN	22.674	
Retinoid-inducible serine carboxypeptidase	Q9HB40	RISC_HUMAN	19.087	
Transcription elongation factor SPT6	Q7KZ85	SPT6H_HUMAN	18.87	
Golgi reassembly-stacking protein 2	Q9H8Y8	GORS2_HUMAN	18.15	
General transcription factor IIH subunit 1	P32780	TF2H1_HUMAN	16.915	
Disintegrin and metalloproteinase domain-containing protein 10	O14672	ADA10_HUMAN	13.324	
Heme oxygenase 1	P09601	HMOX1_HUMAN	11.431	
Nck-associated protein 1-like	P55160	NCKPL_HUMAN	10.686	
Protein phosphatase 1 regulatory inhibitor subunit 16B	Q96T49	PP16B_HUMAN	10.009	
Biotinidase	P43251	BTD_HUMAN	8.577	
UTP--glucose-1-phosphate uridylyltransferase	Q16851	UGPA_HUMAN	8.14	
Fermitin family homolog 3	Q86UX7	URP2_HUMAN	7.582	
Downregulated ≥2 fold				
Glutathione peroxidase 1	P07203	GPX1_HUMAN	0.111	
Protein diaphanous homolog 1	O60610	DIAP1_HUMAN	0.121	
Apolipoprotein E	P02649	APOE_HUMAN	0.174	

Mitochondrial intermediate peptidase	Q99797	MIPEP_HUMAN	0.186
Inorganic pyrophosphatase 2, mitochondrial	Q9H2U2	IPYR2_HUMAN	0.187
Catechol O-methyltransferase domain-containing protein 1	Q86VU5	CMTD1_HUMAN	0.206
Dystonin	Q03001	DYST_HUMAN	0.211
TATA element modulatory factor	P82094	TMF1_HUMAN	0.213
ATP-binding cassette sub-family B member 8, mitochondrial	Q9NUT2	ABCB8_HUMAN	0.217
Ribosome biogenesis protein BOP1	Q14137	BOP1_HUMAN	0.236
Annexin A4	P09525	ANXA4_HUMAN	0.238
Cohesin subunit SA-1	Q8WVM7	STAG1_HUMAN	0.25
Beta-mannosidase	O00462	MANBA_HUMAN	0.252
Cytoskeleton-associated protein 5	Q14008	CKAP5_HUMAN	0.26
Tubulin beta-1 chain	Q9H4B7	TBB1_HUMAN	0.286

<u>Table 2:</u> Combined MALDI and Orbitrap chemoproteomic MS/MS identifications. The protein Erbin is identified as a WA target based on a single SILAC peak (MALDI) and based on quantification of the Orbitrap chemoproteomic data. No fold change value indicates identification according to S in figure 4B.

Protein Name MALDI TOF/TOF and Orbitrap	**UniProtKB Entry**	**UniProtKB Entry Name**	**Fold Change**
Erbin	Q96RT1	ERBIN_HUMAN	Target/ 2.472
Proline-, glutamic acid- and leucine-rich protein 1	Q8IZL8	PELP1_HUMAN	
Calcium load-activated calcium channel	Q9UM00	TMCO1_HUMAN	
Dimethyladenosine transferase 2, mitochondrial	Q9H5Q4	TFB2M_HUMAN	2.283
Heterogeneous nuclear ribonucleoprotein D-like	O14979	HNRDL_HUMAN	2.44
ATP-dependent RNA helicase DDX1	Q92499	DDX1_HUMAN	2.751

MALDI TOF/TOF			
28S ribosomal protein S18c, mitochondrial	Q9Y3D5	RT18C_HUMAN	
Eukaryotic translation initiation factor 5A-1	P63241	IF5A1_HUMAN	
Nucleolar complex protein 2 homolog	Q9Y3T9	NOC2L_HUMAN	
Serrate RNA effector molecule homolog	Q9BXP5	SRRT_HUMAN	0.261
Orbitrap			
Casein kinase I isoform gamma-2	P78368	KC1G2_HUMAN	
Histone deacetylase 6	Q9UBN7	HDAC6_HUMAN	
S-methyl-5'-thioadenosine phosphorylase	Q13126	MTAP_HUMAN	
Ubiquitin carboxyl-terminal hydrolase isozyme L5	Q9Y5K5	UCHL5_HUMAN	4.74
Pre-mRNA cleavage complex 2 protein Pcf11	O94913	PCF11_HUMAN	2.021
Serine/threonine-protein phosphatase 2A 55 kDa regulatory subunit B alpha isoform	P63151	2ABA_HUMAN	2.18
Nuclear cap-binding protein subunit 3	Q53F19	NCBP3_HUMAN	4.112

Table 3: Nineteen proteins were influenced by WA, of which 15 potentially counteract plasma cell dyscrasia (PCD), based on the functions described in table S-6. The binding of WA is assumed to inhibit the protein function. + denotes upregulation, - denotes downregulation.

Protein Name	UniProtKB Entry	Regulation PCD/Regulation WA	Function
Heme oxygenase 1	P09601	-/+	Stress response
Ras-related protein Rab-24	Q969Q5	-/+	Autophagy related processes
Protein kinase C alpha type	P17252	-/+	Serine/threonine-protein kinase
Protein FAM46C	Q5VWP2	-/+	Suggested tumor suppressor
Ras-related protein Rab-4A	P20338	+/-	Vesicular traffic
Signal recognition particle 54kDa protein	P61011	+/-	Transfer presecretory proteins
Annexin A4	P09525	+/-	Exocytosis
Tubulin beta-1 chain	Q9H4B7	+/-	Constituent of microtubules

HLA class I histocompatibility antigen	Q31610	+/WA target	Antigen presentation to the immune system
Histon deacetylase 6	Q9UBN7	No change/WA target	Deacetylates core histones H2A, H2B, H3 and H4
Proteasome subunit beta type-10	P20618	No change/WA target	20S proteasome subunit
Calcium signal-modulating cyclophilin ligand	P49069	No change/WA target	Mobilization of calcium
Proteasome subunit beta type-1	P20618	No change/+	20S proteasome subunit
Proteasome subunit alpha type-2	P25787	+/+	20S proteasome subunit
Exosome complex exonuclease RRP44	Q9Y2L1	Mutation/WA target	Catalytic component RNA exosome complex
C-terminal binding protein 1	Q13363	-/WA target and upregulated	Corepressor of diverse transcription regulators
Protein diaphanous homolog 1	O60610	-/-	Cell morphology and cytoskeletal organization
Rho GTPase-activing protein 1	Q07960	+/+	GTPase activator
Transcription initiation factor IIB	Q00403	-/WA target	General transcription factor

Figures

Figure 1: Molecular structure of Withaferin A (WA) and Withanone (WN). Both molecules have the same chemical brute formula ($C_{28}H_{38}O_6$), but differ in their spatial orientation the hydroxyl and epoxide groups.

Figure 2: WA, but not WN, triggers apoptotic cell death in GC-resistant MM1R cells. A) MM1R cells were treated with 1 µM WN or 1 µM WA at different time points (h), as indicated. Total cell lysates were analyzed by Western blot for assesment of PARP cleavage and GAPDH expression levels. B) MM1R cells were treated with 1 µM dexamethasone and 2 µM WN or 2 µM WA at different time points (h), as indicated. Total cell lysates were analyzed by Western blot for assesment of caspase 3 cleavage and GAPDH expression levels.

Figure 3: MM1R cells were pretreated with WN for 30 minutes at the concentrations indicated. Immediately afterwards, the cells were treated with 0,5 µM WABI for 1 h 30 min and WABI-bound proteins were visualized by Western blot using HRP-conjugated streptavidin.

Figure 4: A) Outline of the SILAC differential expression workflow for identification and quantification of WA-regulated proteins. MM1R cells were grown in light ($^{12}C_6$) – or heavy ($^{13}C_6$) Lys and Arg media, respectively, and either treated with WN (control) or WA. After 2D LC analysis, proteins were identified and quantified by MALDI-TOF-TOF and Orbitrap mass spectrometry. Three possible SILAC ratio combinations were possible in the m/Z spectrum: 1) both peaks have the same intensity, which indicates proteins that do not differentially change their expression. 2) peaks with different intensities due to the protein downregulation after the WA treatment. A fold change ≥ 2 was considered relevant. 3) peaks with different intensities due to the protein upregulation after the WA treatment. A fold change ≥ 2 was considered relevant. B) Outline of the quantitative chemoproteomics workflow with a

forward SILAC labeling strategy. MM1R cells were grown in light ($^{12}C_6$) – or heavy ($^{13}C_6$) Lys- and Arg- containing media and treated as indicated. WA was used as the control treatment, while a biotinylated form of WA (WABI) was used to selectively enrich WA target proteins via a streptavidin pull down. After 2D LC/MS analysis, three types of identifications could be discriminated based on the following: non-specific (NS) identifications are protein interactions with carrier beads and are not related to the initial treatment conditions. Therefore, the MS peaks with the same intensity will be observed. Specific (S) identifications are interactions of WABI-bound target proteins selectively enriched by streptavidin pull down, resulting in single peaks. Additionally, single peaks from light proteins occur, but these are likely due to environmental contaminates (e.g., keratins). Lastly, a combination of specific and non-specific (S + NS) identifications is also possible by quantification of the chemoproteomic data.

Figure 5: Differential plots of all quantified proteins with MALDI (A) and Orbitrap (B) mass spectrometry. Left Y axis = log (fold change) and right Y axis = fold change. The area above the dashed line indicates upregulated proteins (≥ 2-fold) and the area below the solid line indicates downregulated proteins (≥ 2-fold).

Figure 6: A) $C_{38}H_{52}N_2O_8S$ structure of biotinylated WA (WABI). The primary alcohol group at carbon 27 (C27) was replaced by a chain linker and a biotin moiety, and no loss in antitumor activity of WA was observed. B) Western blot detection of caspase-3 cleavage in MM1R cells treated with 1 µM WABI or 1 µM WN. C) Western blot detection of WABI-bound proteins with streptavidin-HRP. MM1R cells were treated with 1 µM WABI for 3 h alone or in combination with an excess DTT (100 mM). Total protein lysates from each condition were analyzed without streptavidin pull down ("INPUT") or submitted to streptavidin pull down ("ELUTION").

Figure 7: A) Top 5 ranked disease and function resulting from the IPA core analysis, with the indication of threshold line corresponding to p < 0,05 (=-log(p-value)). B) Filtering on the 31 types of cancer assigned in the function 'cancer' shows that plasma cell dyscrasia was significantly enriched (p-value = 1.39E-03), with 19 unique molecules. Green = downregulated by WA; red = upregulated by WA; gray =WA target. * denotes a protein that is differentially expressed and targeted by WA. Numbers indicate the log(fold change). C) WB validation of plasma cell dyscrasia-related proteins regulated by WA. For all Western blots, MM1R cells were treated with 1 µM WN or 1 µM WA for 3 h. D) Streptavidin pull down (ELUTION) and WB validation of the WA-PSMB10 association.

Figure 8: A) Top 5 canonical pathways influenced by WA, with the yellow threshold line corresponding to p < 0,05 (= -log(p-value)). Squares indicate the number of proteins within our dataset compared to the total number of proteins for that pathway using the IPA knowledge database. B) WB of anti-ubiquitin shows time- and concentration-dependent accumulation of ubiquitinated proteins after WA treatment.

Figure 9: Withaferin A antitumor effects could be explained by the simultaneous inhibition of proteotoxic and oxidative stress pathways leading to apoptosis. Orange = WA target proteins, green = downregulation, red = upregulation. Proteasome inhibition by WA binding to the PSMB10 subunits results in accumulation of ubiquitinated proteins. A rescue pathway via Nrf1 will result in upregulation of proteasome subunits (PSMB1 and PSMA2). If unresolved, ubiquitinated proteins will aggregate in large complexes (aggresomes) which are degraded by lysosome via autophagy. Simultaneous with proteasome inhibition, the autophagy pathway is impaired by targeting HDAC6 and downregulation of ANXA4. A third proteotoxic antitumor mechanism of WA is proposed by the binding of WA to HSF-1 which impairs heat shock protein synthesis and subsequent protein folding control. This results in aggregation of misfolded proteins which must be degraded by the autophagy pathway. Besides proteotoxic stress, WA is able to induce oxidative stress

via Nrf2 and the upregulation of HMOX1. Eventually, the combined action of blocking all cellular stress rescue pathways will result in apoptotic cell death of the cancer cells.

Conflict of interest: The authors declare no potential conflicts of interest.

Significance

Multifunctional antitumor compounds are of great potential since they reduce the risk of multidrug resistance in chemotherapy. Unfortunately, characterization of all protein targets of a multifunctional compound is lacking. Therefore, we optimized an SILAC quantitative chemoproteomics workflow to identify the potential protein targets of Withaferin A (WA), a natural multifunctional compound with promising antitumor properties. To further understand the antitumor mechanisms of WA, we performed a differential protein expression analysis and combined the altered expression data with chemoproteome WA target data in the highly curated Ingenuity Pathway database. We provide a first global overview on how WA kills multiple myeloma cancer cells and serve as a starting point for further in depth experiments. Furthermore, the combined approach can be used for other types of cancer and/or other promising multifunctional compounds, thereby increasing the potential development of new antitumor therapies.

Highlights

- Quantitative chemoproteomics identifies 208 Withaferin A targets
- 143 proteins were altered in response to Withaferin A treatment
- Withaferin A targets specific myeloma gammopathy protein networks
- Withaferin A inhibits proteasome, autophagy and unfolded protein stress response

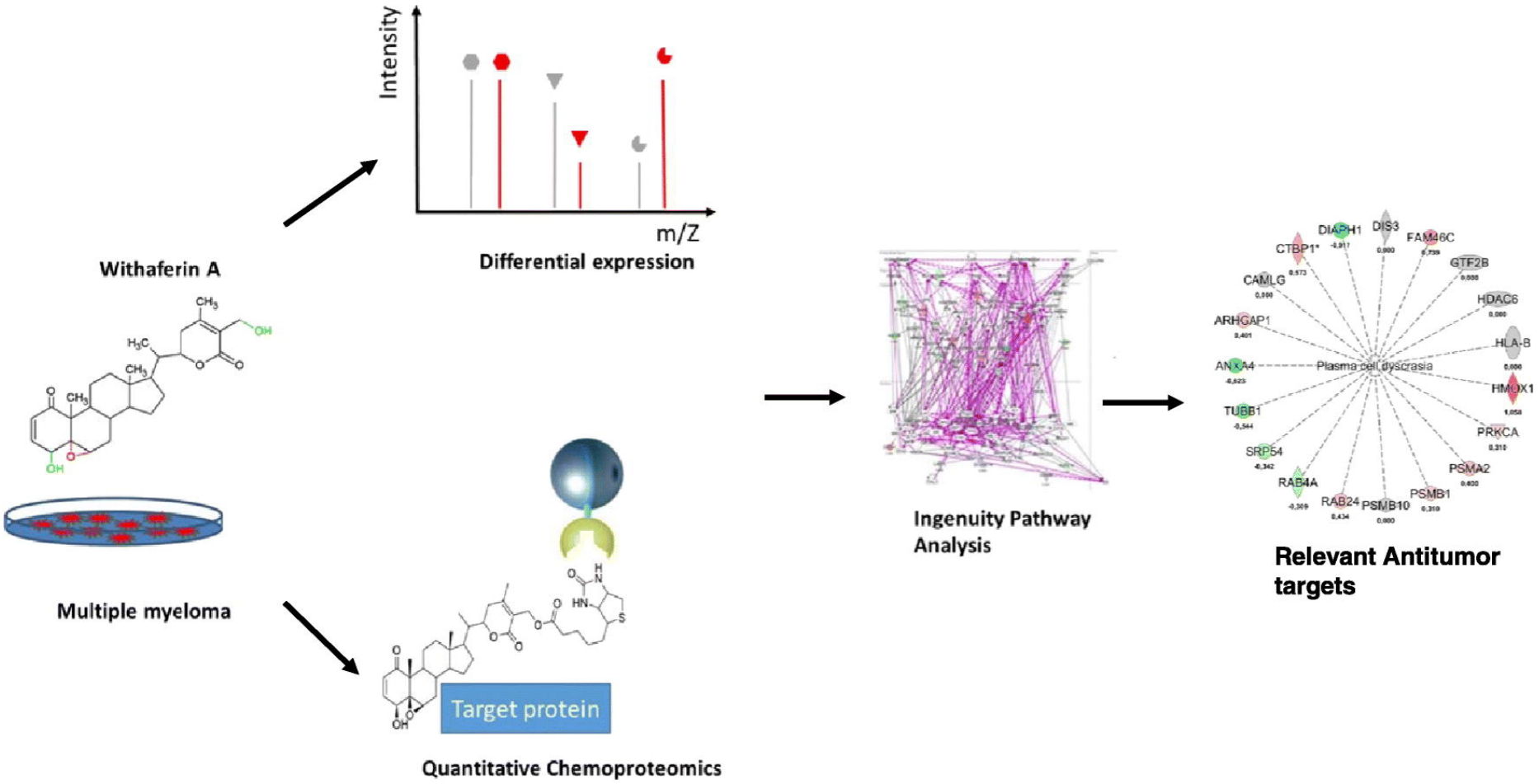

Graphics Abstract

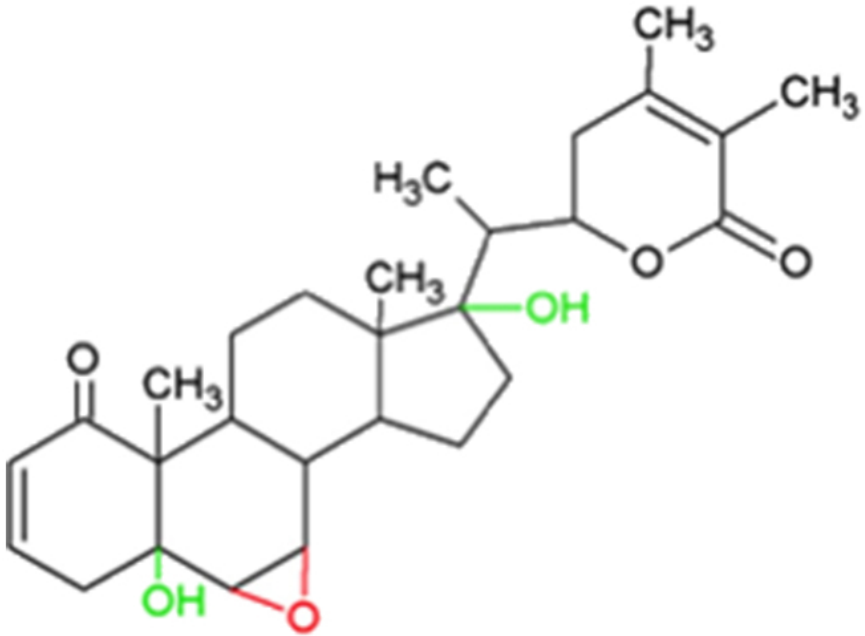

Withanone

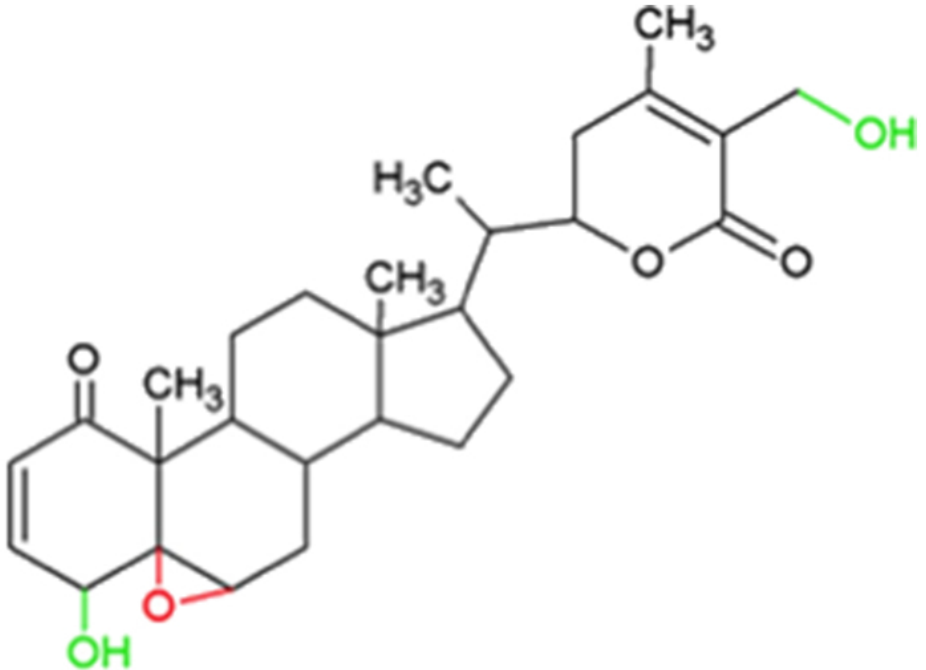

Withaferin A

Figure 1

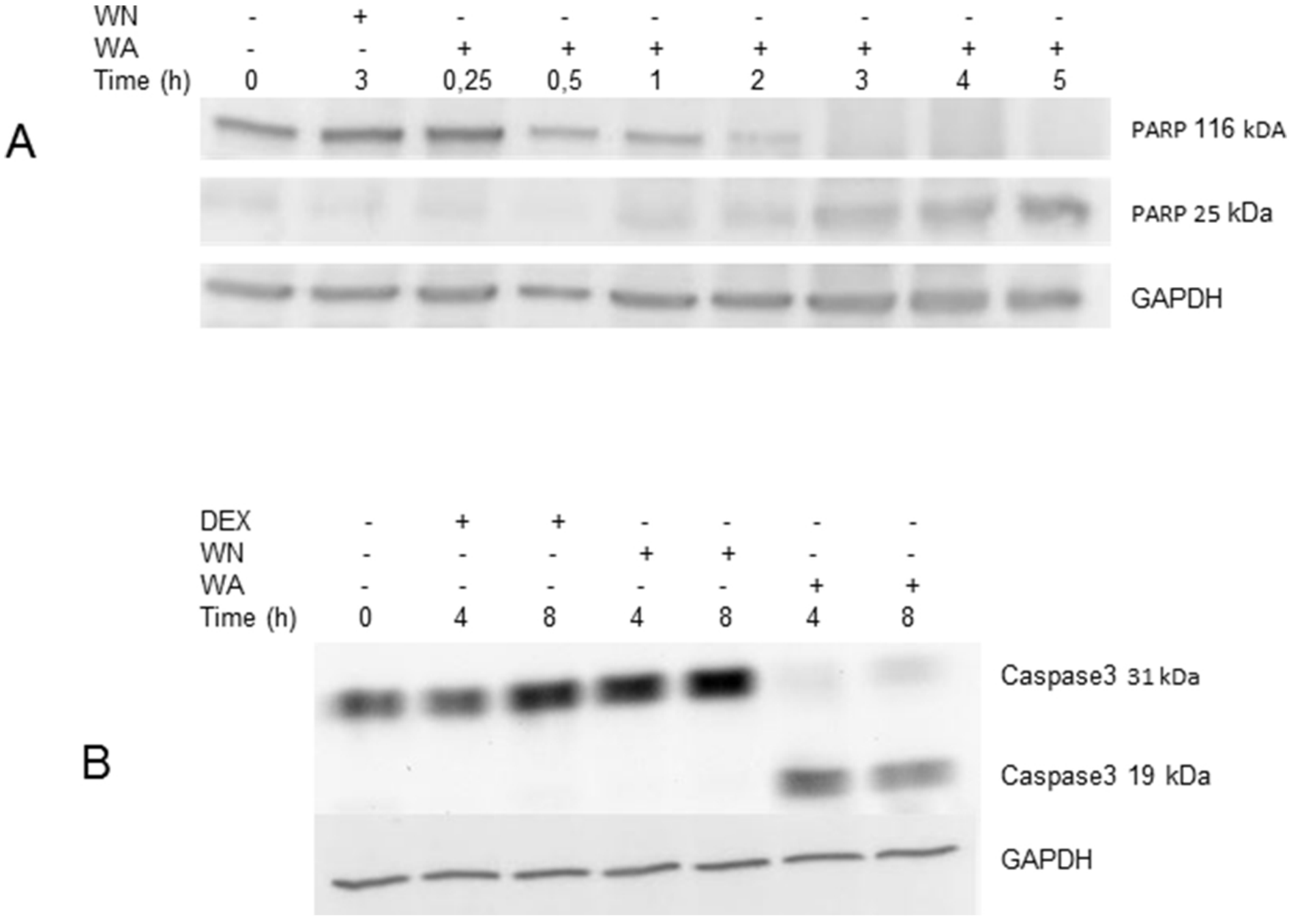
WN - + - - - - - - -
WA - - + + + + + + +
Time (h) 0 3 0,25 0,5 1 2 3 4 5
A
PARP 116 kDA
PARP 25 kDa
GAPDH
DEX - + + - - - -
WN - - - + + - -
WA - - - - - + +
Time (h) 0 4 8 4 8 4 8
B
Caspase3 31 kDa
Caspase3 19 kDa
GAPDH

Figure 2

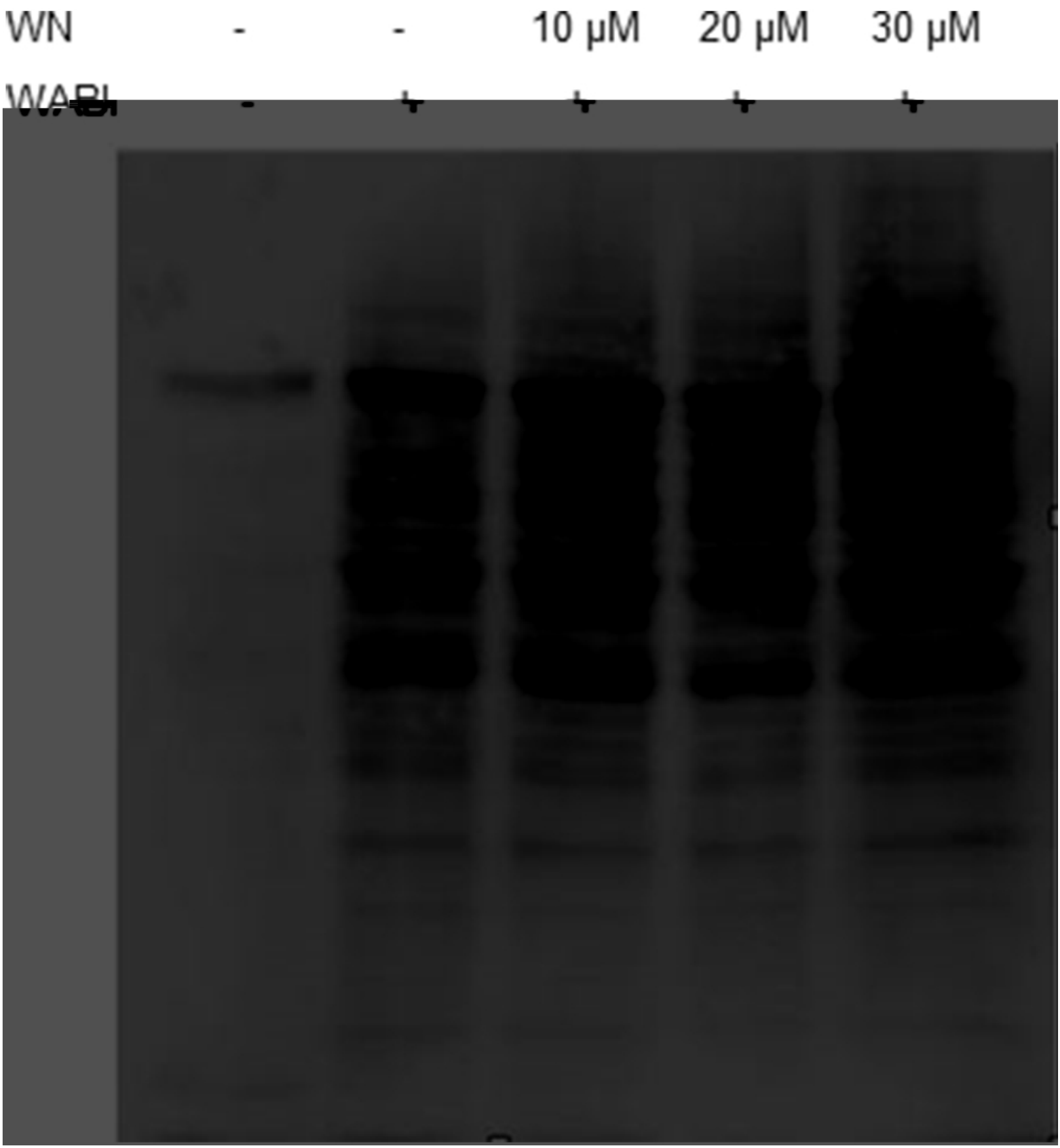

Figure 3

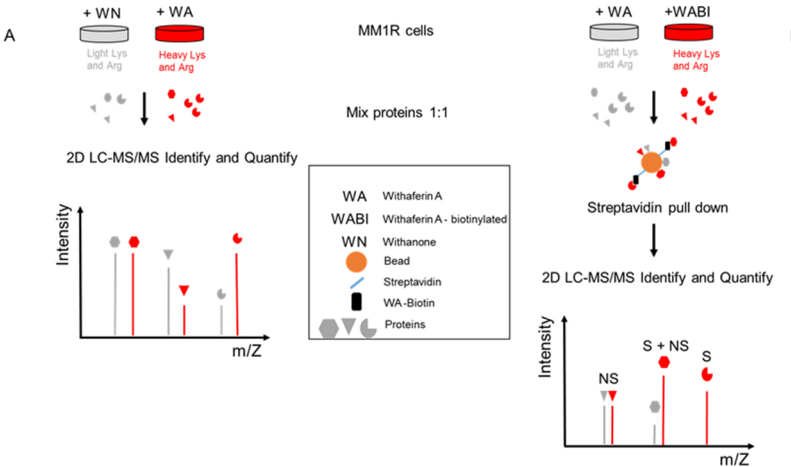

	Chemoproteomics		Differential expression		
	WA	WABI	WN	WA	
rd	$^{12}C_6$ L-Lysine and $^{12}C_6$ L-Arginine	$^{13}C_6$ L-Lysine and $^{13}C_6$ L-Arginine	$^{12}C_6$ L-Lysine and $^{12}C_6$ L-Arginine	$^{13}C_6$ L-Lysine and $^{13}C_6$ L-Arginine	Forwa
se	$^{13}C_6$ L-Lysine and $^{13}C_6$ L-Arginine	$^{12}C_6$ L-Lysine and $^{12}C_6$ L-Arginine			Rever

C

Figure 4

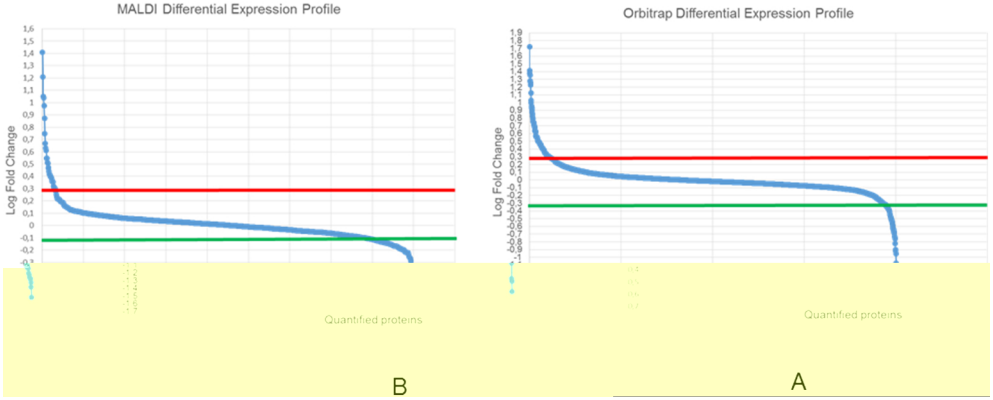
MALDI Differential Expression Profile
Log Fold Change
Quantified proteins
B
Orbitrap Differential Expression Profile
Log Fold Change
Quantified proteins
A

Figure 5

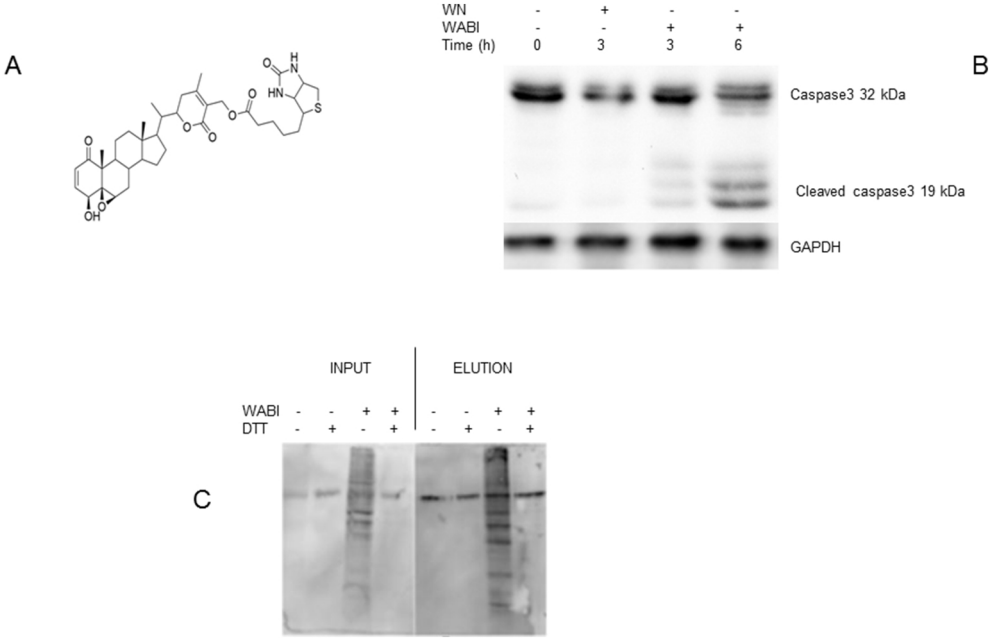
A
B
WN - + - -
WABI - - + +
Time (h) 0 3 3 6
Caspase3 32 kDa
Cleaved caspase3 19 kDa
GAPDH
C
INPUT
ELUTION
WABI - - + + - - + +
DTT - + - + - + - +

Figure 6

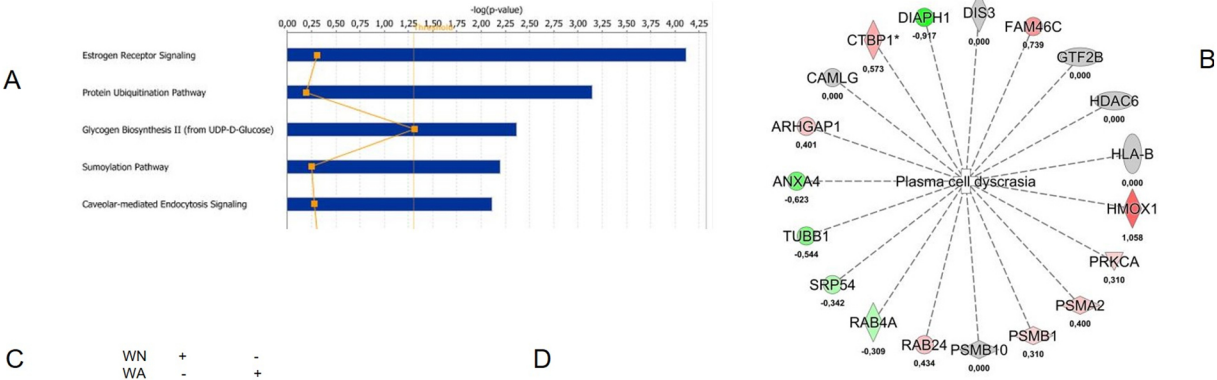
A
-log(p-value)
0,00 0,25 0,50 0,75 1,00 1,25 1,50 1,75 2,00 2,25 2,50 2,75 3,00 3,25 3,50 3,75 4,00 4,25
Estrogen Receptor Signaling
Protein Ubiquitination Pathway
Glycogen Biosynthesis II (from UDP-D-Glucose)
Sumoylation Pathway
Caveolar-mediated Endocytosis Signaling
B
Plasma cell dyscrasia
DIAPH1 -0,917
DIS3 0,000
FAM46C 0,739
CTBP1* 0,573
GTF2B 0,000
CAMLG 0,000
HDAC6 0,000
ARHGAP1 0,401
HLA-B 0,000
ANXA4 -0,623
HMOX1 1,058
TUBB1 -0,544
PRKCA 0,310
SRP54 -0,342
PSMA2 0,400
RAB4A -0,309
RAB24 0,434
PSMB10 0,000
PSMB1 0,310
C
WN + -
WA - +
PSMB1
ANXA4
HMOX1
GAPDH
D
INPUT
ELUTION
WA + - + -
WABI - + - +
PSMB10
GAPDH

Figure 7

A

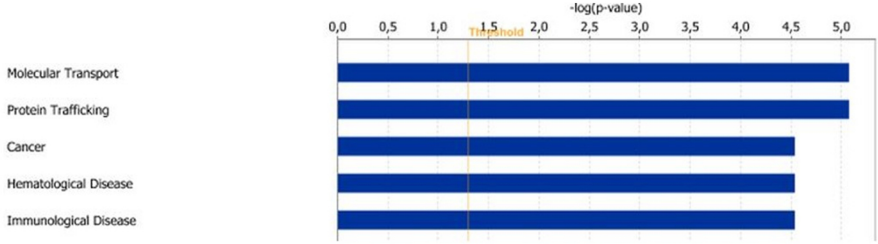
-log(p-value)
0,0
0,5
1,0
1,5
2,0
2,5
3,0
3,5
4,0
4,5
5,0
Threshold
Molecular Transport
Protein Trafficking
Cancer
Hematological Disease
Immunological Disease

B

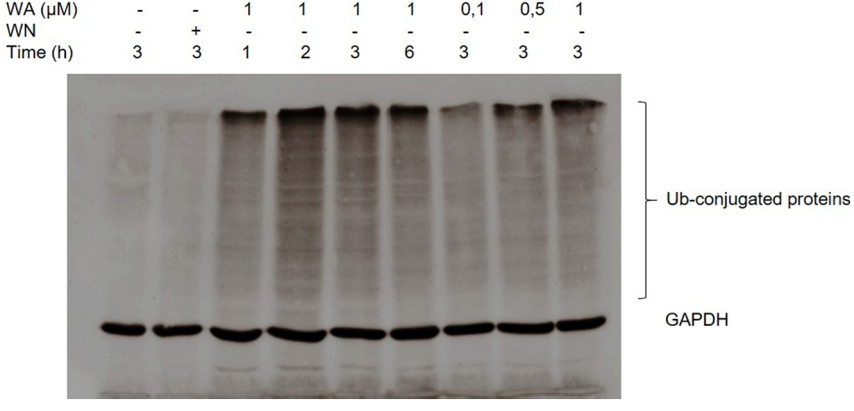
WA (μM) - - 1 1 1 1 0,1 0,5 1
WN - + - - - - - - -
Time (h) 3 3 1 2 3 6 3 3 3
Ub-conjugated proteins
GAPDH

Figure 8

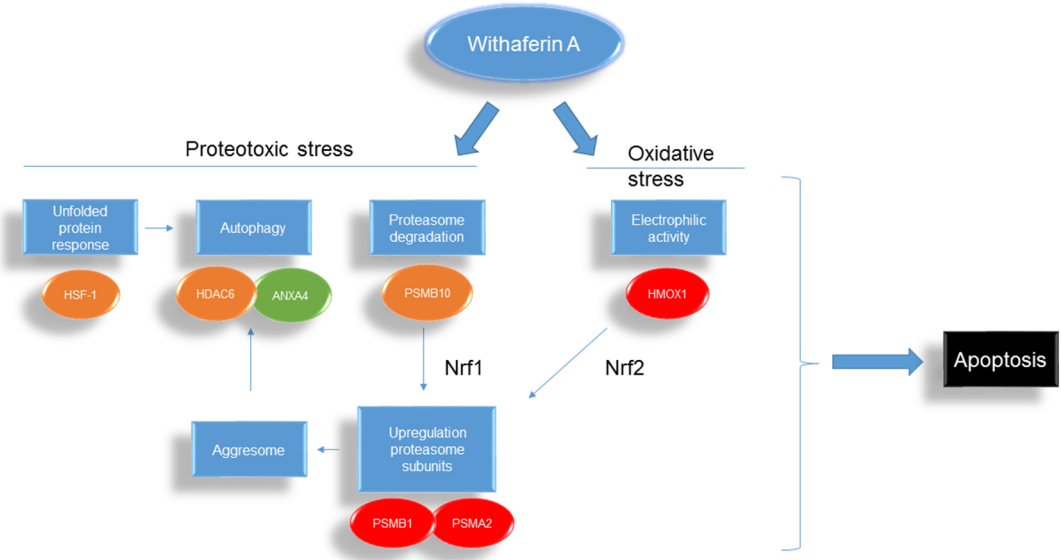
Withaferin A
Proteotoxic stress
Oxidative stress
Unfolded protein response
Autophagy
Proteasome degradation
Electrophilic activity
HSF-1
HDAC6
ANXA4
PSMB10
HMOX1
Nrf1
Nrf2
Apoptosis
Aggresome
Upregulation proteasome subunits
PSMB1
PSMA2

Figure 9

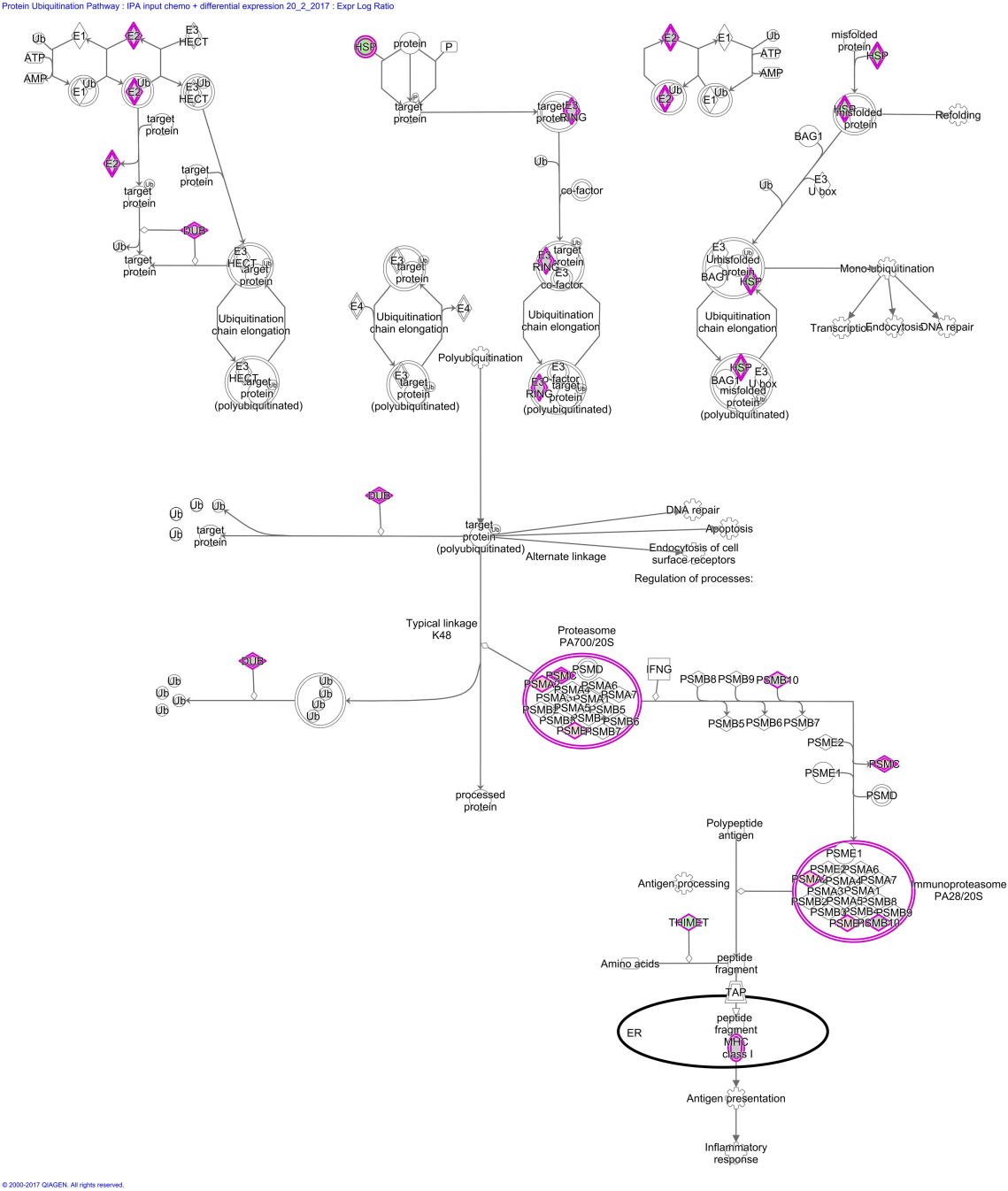
Protein Ubiquitination Pathway : IPA input chemo + differential expression 20_2_2017 : Expr Log Ratio
Ub
E1
E2
E3
HECT
ATP
AMP
target protein
DUB
Ubiquitination chain elongation
(polyubiquitinated)
HSP
P
co-factor
RING
E4
Polyubiquitination
misfolded protein
Refolding
BAG1
U box
Unfolded protein
Mono-ubiquitination
Transcription
Endocytosis
DNA repair
DNA repair
Apoptosis
Endocytosis of cell surface receptors
Regulation of processes:
Alternate linkage
Typical linkage K48
Proteasome PA700/20S
PSMC
PSMD
PSMA
PSMB
IFNG
PSMB8
PSMB9
PSMB10
PSMB5
PSMB6
PSMB7
PSME2
PSME1
processed protein
Polypeptide antigen
Antigen processing
Immunoproteasome PA28/20S
THIMET
Amino acids
peptide fragment
TAP
ER
MHC class I
Antigen presentation
Inflammatory response
© 2000-2017 QIAGEN. All rights reserved.

Figure 10